Journal of Japan Association for Earthquake Engineering, Vol. 21, No. 6, 2021

MECHANISM OF THE GRABENS THAT FORMED IN THE ASO CALDERA DURING THE 2016 KUMAMOTO EARTHQUAKE

Susumu YASUDA[1], Naoto OHBO[2], Masanobu SHIMADA[3], Tatsuro CHIBA[4], Hideo NAGASE[5], Satoshi MURAKAMI[6], Shigeki SENNA[7], Naoko KITADA[8] and Keisuke ISHIKAWA[9]

[1] Honorary Member, Dr. Eng., Professor Emeritus, Tokyo Denki University, Saitama, Japan, yasuda@g.dendai.ac.jp
[2] Member, Dr. Eng., Senior Research Adviser, Association for the Development of Earthquake Prediction, Tokyo, Japan, ohbo@adep.jp
[3] Dr. Eng., Professor, Tokyo Denki University, Saitama, Japan, shimada@g.dendai.ac.jp
[4] M. Sc., Fellow Director, Asia Air Survey Co., Ltd., Kanagawa, Japan, chiba@ajiko.co.jp
[5] Member, Dr. Eng., Professor Emeritus, Kyushu Institute of Technology, Fukuoka, Japan, nagase.hideo631@mail.kyutech.jp
[6] Ph. D., Professor, Fukuoka University, Fukuoka, Japan, sato4murakami@fukuoka-u.ac.jp
[7] Member, Dr. Eng., Principal Researcher, National Research Institute for Earth Science and Disaster Resilience, Ibaraki, Japan, senna@bosai.go.jp
[8] Dr. Sc., Executive Director, Geo-Research Institute, Osaka, Japan, kitada@geor.or.jp
[9] Member, Dr. Eng., Associate Professor, Tokyo Denki University, Saitama, Japan, ishikawa@g.dendai.ac.jp

ABSTRACT: During the 2016 Kumamoto Earthquake, many special belt-like subsidences called “grabens” occurred in the Aso Caldera, and houses were severely damaged. According to the measurement results of SAR, a horizontal displacement of 2 to 3 m was generated in the area where the grabens occurred. A lake was formed in this area around 9,000 years ago. A soil investigation showed that the bottom of the old lake was bowl-shaped, and a special clay was deposited there. A residual deformation analysis showed that the soft clay flowed due to the earthquake, causing the grabens at the ground surface.

Keywords: *Kumamoto Earthquake*, *Graben*, *Aso Caldera*, *Lake deposit*

1. INTRODUCTION

The 2016 Kumamoto Earthquake caused geotechnical damage, such as liquefaction, the failure of a natural slope, the deformation of filled residential land, the deformation of a river embankment, the failure of a road and reservoir embankment, and a crack on the ground surface due to fault, over a wide range from Kumamoto Prefecture to Oita Prefecture. This damage had occurred during past earthquakes, but during the Kumamoto Earthquake, unusual belt-like subsidences called “grabens” occurred in the Aso Caldera, as shown in Photo 1. Due to the steps created by the subsidences, several houses were

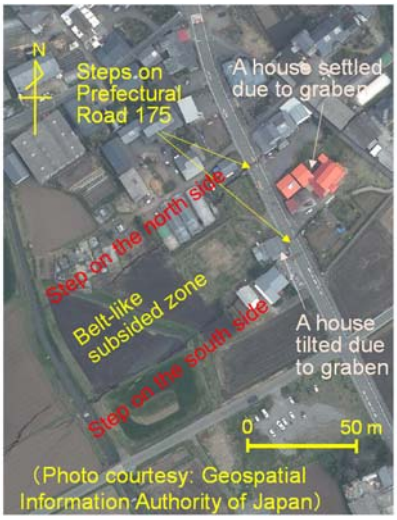

Photo 1 A graben in the Kario district

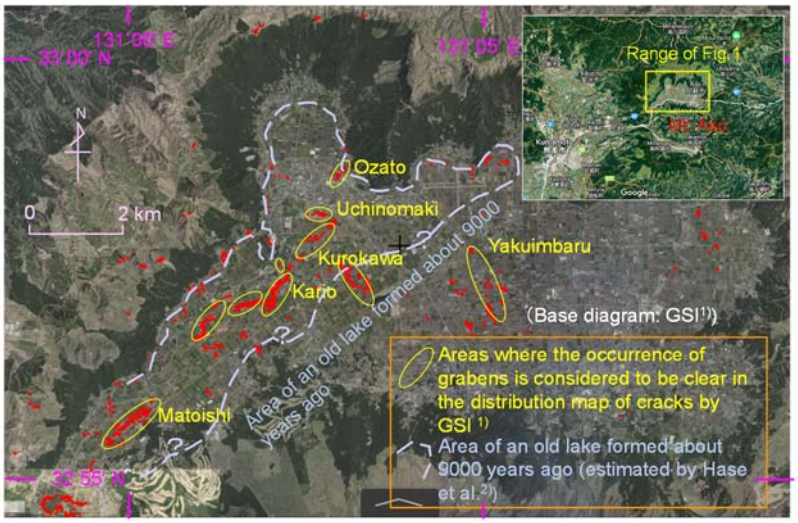

Fig. 1 Estimated areas where grabens occurred in the Aso Valley

deformed into a guillotine shape, and those with strong foundations tilted without breaking their glass windows. Not only roads, but also buried pipes, river revetments, and agricultural lands were damaged.

A caldera of about 25 km in the north-south direction and about 18 km in the east-west direction was formed in Aso, and central cones were formed inside. For this reason, there were caldera lowlands in both the north and south, and the northern part is called Asodani (Aso Valley). As shown in Fig. 1, grabens occurred over a wide area of about 10 km × 2 km in the western half of Aso Valley. The grabens were several tens of m in width, one to two m in depth, and several tens to several hundred m in length. Most of the grabens occurred in the northeast-southwest direction, and some in the northwest-southeast direction. Figure 2 shows a geological map of Aso Valley[3]. Caldera bottom sediment is deposited in the northern half of Aso Valley, and alluvial fan deposits from the central cones are deposited in the southern half. The grabens in the northeast-southwest direction are positioned in the former range, and the grabens in the northwest-southeast direction are positioned in the latter. Within the former range, the Kuro River runs from the Ozato district in the northeast to the Matoishi district in the southwest. The altitude is about 480 m in the Ozato district and about 470 m in the Matoishi district, and the gradient from northeast to southwest is about 0.1%, which is almost flat. Even in the orthogonal direction, the maximum slope is around 0.5% within the range where the caldera bottom sediment is distributed, and the slope is small.

Such peculiar belt-like subsidences have not been reported from domestic and foreign earthquakes. Possible causes of the occurrence were considered to be as follows: (1) a normal fault type depression due to the north-south tensile force related to the Beppu-Shimabara subsided zone, (2) a strike-slip fault that continues from the Futagawa fault, (3) liquefaction, and (4) special geological conditions at the edge of the caldera. However, the causes could not be determined just from the resulting damage. Therefore, the authors decided to study the mechanism of the grabens with the support of the JSPS KAKENHI. Research started in April 2017, and a detailed investigation of the ground deformation, an examination of the specificity of ground motion, a detailed soil investigation and geophysical exploration, and a damage reproduction analysis were conducted over three years to elucidate the mechanism of damage.

2. POST-EARTHQUAKE RESEARCH ON THE GRABENS CONDUCTED SHORTLY AFTER THE EARTHQUAKE AND SIMILAR DISASTER CASES IN PAST EARTHQUAKES

2.1 Post-earthquake research on ground deformation in the Aso Valley conducted shortly after the Kumamoto Earthquake

Regarding the ground deformation caused by the 2016 Kumamoto Earthquake, not only field

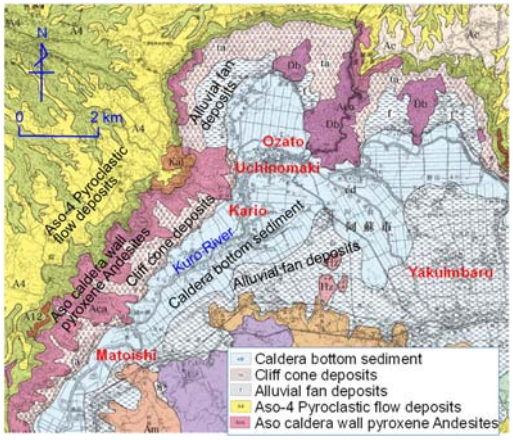

Fig. 2 Geological map of Aso Valley[3)]

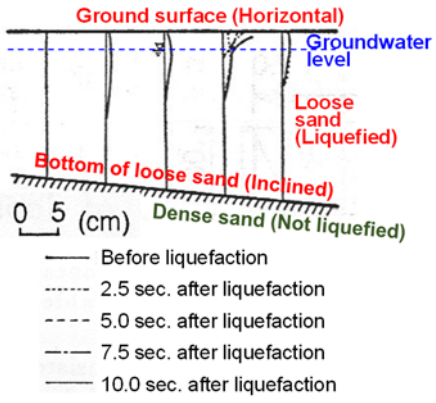

Fig. 3 Liquefaction-induced ground flow observed in small shaking table[7)]

reconnaissance but also research using aerial photographs and satellite images has been conducted by several organizations. The main research area was Kumamoto City and its surroundings, but the following research was also conducted in the Aso Valley.

The Geospatial Information Authority of Japan (GSI) conducted a three-dimensional displacement analysis using synthetic aperture radar (SAR) data from satellites before and after the earthquake, and found that large horizontal displacements in the north-northwest direction occurred in the Uchinomaki, Kario and Matoishi districts of the Aso Valley (Fujiwara et al.[4)]). The displacement at Uchinomaki was 2.6 m and that at Matoishi was 3.8 m, which were larger than the displacement at the Futagawa fault (maximum 2 m), which caused the Kumamoto Earthquake. Saturated silty lake deposits with low penetration resistance are thickly deposited in this area, and the ground surface is tilted 0.16 to 0.6% in the direction of displacement. It was estimated that part of the soil layer deeper than 30 m liquefied and moved in the north-northwest direction, causing graben-type cracks.

Tsuji et al.[5)] showed that the ground surface was displaced in the northwest direction from the SAR data and further revealed that the wells of the Uchinomaki hot spring were bent by the earthquake. They showed that the bending depth was around 50 m, and the hot spring water accumulated near this depth. In addition, a silt layer is deposited on the upper part of the impermeable layer, a gravel layer is deposited on the lower part, and the ground surface is almost flat, with an inclination of 0.06 degree. It was estimated that the pore water pressure of the gravel layer increased due to the foreshock and the main shock, and the layer slipped due to the seismic force.

2.2 Similar damage from past earthquakes

Fujiwara et al.[4)] and Tsuji et al.[5)] presumed that the grabens occurred due to local horizontal displacement, but the mechanism of horizontal displacement they considered differs slightly. In addition, as mentioned above, there are several possible mechanisms for the occurrence of grabens. Therefore, as part of our research, the authors conducted a preliminary study on the possible mechanism based on similar damage caused by past earthquakes.

(1) Normal fault-type depression due to the north-south tensile force related to the Beppu-Shimabara subsided zone

The northeastern end of the area where the grabens occurred extends to the Ozato area and not to the east of this area. In addition, the Geographical Survey Institute and Tsuji et al. stated in their research that the possibility of depression was low because grabens occurred only in areas where a large amount of ground surface displacement had been locally generated.

(2) The right-lateral stepping fault following the Futagawa fault

The right-lateral Futagawa fault that caused the main shock of the Kumamoto Earthquake on April 16 extended east to Minamiaso Village. However, it does not seem that the fault continued beyond this

village and caused grabens. In addition, the subsidence that occurred in stepping faults was usually not belt-like subsidence. Therefore, the possibility of the right-lateral stepping fault following the Futagawa fault causing grabens is low.

(3) Soil liquefaction

When liquefaction occurs, settlement occurs due to volume compression. In addition, sloped ground flows and is displaced in the horizontal direction. The depressions of the grabens were subsidences as if the ground had been cut. If liquefaction had caused these depressions, the boundary of the liquefied area must have been discontinuous. However, it is considered that such discontinuous ground formation is rare in natural ground. A typical example of liquefaction-induced flow on sloping ground occurred on the gentle slopes of the sand dunes of Noshiro City during the 1983 Nihonkai-Chubu Earthquake, which caused a displacement of up to 5 m (Hamada et al.[6]). Sand volcanoes, which indicate liquefaction, also occurred everywhere, and the ground surface was tilted by about 2 to 3%. However, since the 1964 Niigata Earthquake caused flow even on almost flat ground, two of the authors investigated the effects of the inclination angles of the ground surface and the bottom of the liquefaction layer in a shaking table experiment (Yasuda et al.[7]). Figure 3 shows the test results when the bottom of the liquefaction layer was inclined and the ground surface was flat. The vertical line shows the deformed state of Japanese soft noodles placed vertically between the glass surface of a soil container and the soil in the container. As can be seen in the figure, even if the ground surface is flat, a small horizontal displacement occurs, and when the ground surface is also tilted, a larger displacement occurs. In addition, instead of forming a slip surface, shear deformation occurred as a whole, causing horizontal displacement. Therefore, if the bottom of the liquefaction layer is tilted, it is considered that shear deformation occurs due to the rapid decrease in shear stiffness due to liquefaction. It is possible that the same phenomenon might occur in these grabens, but it is necessary to conduct detailed soil tests to discover whether the soil in Aso also experienced a sharp decrease in shear stiffness due to the earthquake.

(4) Peculiar soil layer composition at the edge of the caldera

During the 1985 Michoacan, Mexico Earthquake, houses and roads were damaged along a line in Guzman City (Mimura et al.[8]). It was located on the edge of a caldera, and there was a linear step of 40 to 50 cm. Microtremor observations revealed that the periodic characteristics changed suddenly across this line, and it was estimated that the thickness of the soil layer deposited on the bottom of the caldera changed suddenly. Since the area targeted in this study is also close to a caldera edge, it is possible that the grabens might have occurred due to the peculiar soil layer composition.

As described above, mechanisms (3) and (4) might have caused the grabens. In order to clarify which mechanism was more likely, the authors conducted the following investigations and analyses: i) investigation of damage, ii) investigation of characteristics of seismic motion, iii) soil investigation and soil test, iv) reproduction analysis based on them.

3. DETAILED INVESTIGATION OF DAMAGE AND GROUND DEFORMATION

3.1 Judgment of the sites where grabens occurred

Immediately after the Kumamoto Earthquake, the GSI[1] read the crack distribution on the ground surface using aerial photographs and published the crack distribution map shown in Fig. 1. The authors conducted field surveys of the locations of the cracks on this map and judged that a graben had occurred at a location where a belt-like subsidence with a depth of 1 to 2 m, a width of several tens of meters, and a length of several tens to several hundreds of meters had occurred. The field survey started on the afternoon of April 16, when the main shock of the Kumamoto Earthquake occurred, and one of the authors conducted a field survey of the Matoishi and the Kario districts on the same night and found a clear depression that obstructed the passage of vehicles. In addition, two of the authors conducted a field survey of the entire Aso Valley on April 24, and confirmed grabens in almost all districts other than the Yakuimbaru district. Furthermore, the Yakuimbaru district was surveyed one year later. Based on the above field surveys, it was judged that grabens occurred in the areas surrounded by ellipses in Fig.1. However, grabens may have occurred in other places.

3.2 Overview of disasters in each district

Of the graben occurrence areas shown in Fig. 1, detailed maps showing the locations of grabens and structural damage caused by them in the Ozato, Uchinomaki, Kario, and Matoishi districts are shown in Figs. 4 to 6. As a result of the investigation, it was found that the mechanism of occurrence of the graben at Yakuimbaru is different from the mechanism in these other areas, so it will be described later in

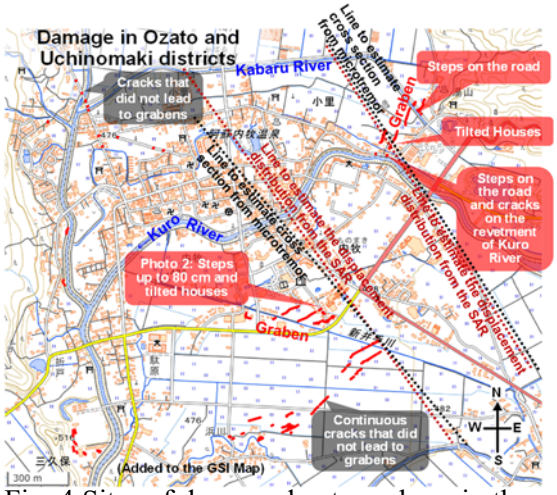

Fig. 4 Sites of damage due to grabens in the Ozato and Uchinomaki districts

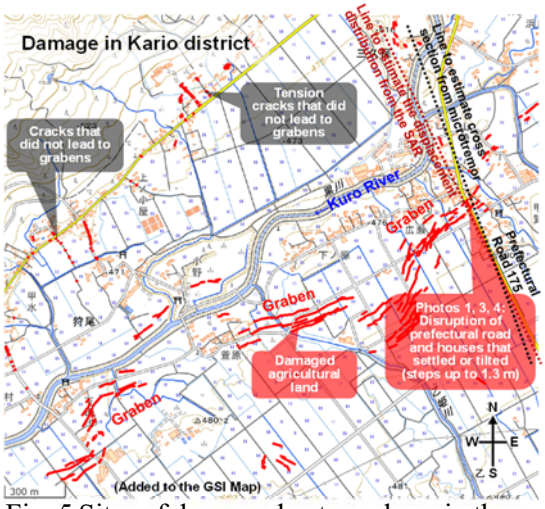

Fig. 5 Sites of damage due to grabens in the Kario district

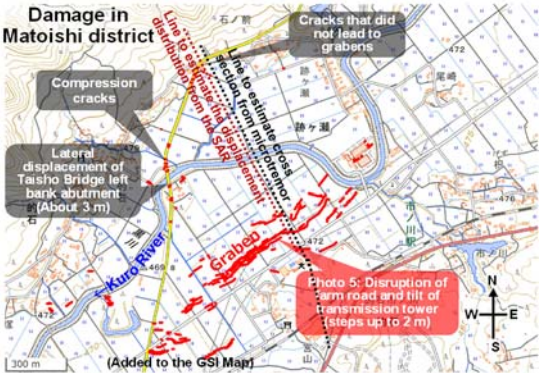

Fig. 6 Sites of damage due to grabens in the Matoishi district

Photo 2 Damage in the Uchinomaki district

Photo 3 Damage in the Kario district

Photo 4 North side of the graben in the Kario district

Photo 5 Damage in the Matoishi district

Photo 6 Ejected sands on agricultural land

Photo 7 Damage in the Yakuimbaru

Appendix 1.

In the Ozato district, grabens occurred in agricultural and residential areas. In the residential area, wooden houses were deformed and tilted due toward the grabens. In addition, cracks were formed in the concrete block revetment of the Kuro River, and a step of about 20 cm was created on a road. In the Uchinomaki district, as shown in Photo 2, a graben caused a step of up to 80 cm in the residential area, and the houses built on the step were greatly inclined. In the Kario district, a graben, as shown in Photo 1, occurred from the residential area to the agricultural land. As shown in Photo 3, the prefectural road was cut off due to the occurrence of a step of up to 1.3 m, a house with a red roof located in the graben sank without deformation, while a house located on the boundary of subsided land was deformed. As shown in Photo 4, a vending machine installed in the graben was undamaged, not tilted or rotated. The damage to the residential area in this district was enormous, and the agricultural land extending further southwest was also severely damaged by the grabens and cracks. Photo 5 was taken in the Matoishi district facing southeast. Here, a large step of up to about 2 m occurred, and a transmission tower was tilted in addition to the damage to the agricultural land.

When the survey was conducted on April 24, sand volcanoes were found in some parts of the agricultural land in Aso Valley, as shown in Photo 6. However, no sand volcanoes were found in the grabens. Since the field survey in Yakuimbaru was conducted about a year after the earthquake, the situation immediately after the earthquake is unknown, but even so, as shown in Photo 7, a graben in the north-south direction remained.

3.3 Detailed survey based on hearings with inhabitants

In addition to the above field reconnaissance, with the cooperation of the inhabitants and Aso City, the authors conducted hearings on the damage in the Kario, Uchinomaki, and Ozato districts. Hearings were conducted twice, in the Kario and Uchinomaki districts on May 21, 2017, and in the Kario, Ozato and Uchinomaki districts on August 19, 2017. Hearing items were (1) damage to residential land and agricultural land (subsidence, steps, cracks, water and sand spew out), (2) damage to houses (foundation type, foundation damage, damaged date and time, the ground had been improved or not), (3) damage due to shaking (feeling of shaking, tipping of furniture, noise of the ground, falling of nearby gravestones), (4) changes in well water, and (5) whether deformation had progressed after the earthquake.

An inhabitant of the Kario district investigated the ground deformation in detail and drew a crack distribution map. Comparing this with the crack distribution map prepared by the GSI, it was found that cracks also occurred in the Z3 zone in Fig. 7. In addition, warm water spouted in the Z5 zone due to the earthquake and continued to spout after that. It is said that grabens did not occur during the foreshock on April 14, but occurred during the main shock on April 16 at midnight. According to two people in the Z1 zone, where a large graben occurred, as shown in Fig. 7, i) houses sank quickly without much shaking, and ii) lanterns and furniture did not tip over and the window glass did not break, iii) a crack with a width of about 50 cm occurred, and when a long stainless-steel rod was inserted into it, the rod penetrated about 6 m. On the other hand, two people in the Z3 zone, where the depth of subsidence was not so deep but many cracks occurred, said that i) they were pushed up at the beginning of the earthquake and then shaken sideways, and ii) TVs and lanterns tipped. It seems that the state of the shaking was slightly different even within the Kario district. According to inhabitants in the Z2 zone, there is a hard

Fig. 7 Crack distribution map

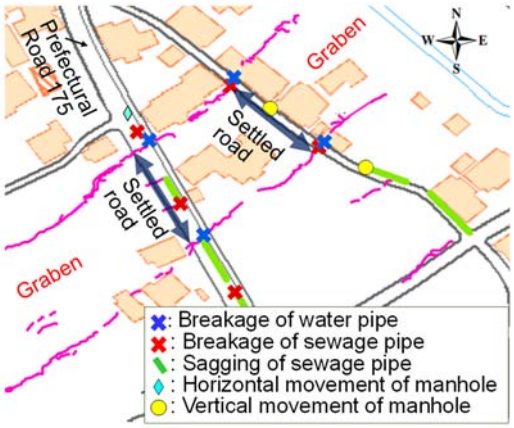

Fig. 8 Damage to water and sewage facilities

sandy soil layer called “Toga” on the surface of the ground, on which houses have been built since ancient times. And he estimates that the houses tilted due to the break of the Toga during earthquake. In addition, according to inhabitants of the Z1 zone, ground deformation has not progressed after the earthquake.

In the Ozato and Uchinomaki districts, one inhabitant of the area where a graben occurred testified, i) it felt that the house suddenly fell and the ceiling fell, ii) the TV on the second floor slipped a little, and iii) the house fell straight down by about 50–60 cm. An inhabitant who was on the second floor of a home at the boundary of a graben testified, i) vertical shaking was intense, and ii) the house tilted with uneven subsidence of up to 12 cm. In addition, an inhabitant living outside the graben testified, i) a violent tremor pushed up the house with noise, but a household Shinto altar did not move, and ii) the house was undamaged although the field next to the house subsided. The boundary of this graben corresponds to the place where the bottom surface of the old lake is steep and the seismic motion is likely to have been amplified. Therefore, it is considered that the shaking was very intense, as will be described later.

3.4 Collection of data on the damage to underground pipelines

According to the data on damage to the water supply and sewerage compiled by Aso City, the damage was concentrated in the districts of Ozato, Uchinomaki, Kario, and Matoishi. Figure 8 shows the locations of damage in the Kario district. Water pipes and a sewer pipe were broken at the boundaries of a graben, probably due to the occurrence of sharp steps. In addition, sewer pipes sagged and manholes moved vertically in the section of subsided ground.

3.5 Measurement of ground displacement by interferometric synthetic aperture radar (SAR)

The amount of crustal movement in the northern part of the Aso Caldera area was measured by interferometric analysis of the SAR data, which were acquired in three different directions and two different timings for each: before and after the earthquake, by JAXA’s Synthetic Aperture Radar (PALSAR-2) of the land observation satellite No. 2 (ALOS-2, DAICHI-2). PALSAR-2 has a long radar wavelength of about 24 cm, and its signal penetrates the vegetation on the surface of the earth to some extent, and thus enables the direct measurement of the distance between the satellite and the surface of the earth. The image resolution is as high as about 3 m, and observes about 50 km square area, which is wide sufficient to cover the caldera topography of Mt. Aso. ALOS-2 is operated regularly and periodically to observe all over Japan in order for the quick change detection at the disaster event and provide the amount of surface displacement immediately when an earthquake occurs. During the Kumamoto Earthquake 2016, observations were made multiple times from three azimuthal directions, and it effectively observed the surface deformation during the foreshock on April 14 and the main shock on April 16. By the InSAR processing of the three image pairs at different directions, the deformation

vector of the ground surface that occurred during this period was calculated. In detail, all six SAR images were created as single-look-complex data from the SAR data using the precise orbit data, and three images are prepared for the before the shock and three are after the shock. Then, differential SAR interferometry and unwrapping processing were performed in each direction, and the amount of line-of-sight change for each pixel on the ground was calculated. As the topographical data, the 10 m mesh digital elevation model (DEM) data of GSI and the geoid model EGM96 were used. Then the displacement vector (East, North, Up components) of the ground surface deformation was obtained by solving the simultaneous equations on the three radar line-of-sight vector and the InSAR displacements. While the SAR data is normally affected by the atmosphere and ionospheric variation, the processed InSAR data were further corrected for filtering out the longer frequency behaivor which corresponds to those variation. The calculated displacement was calibrated using the data collected at the GNSS station (960703) in Aso (GSI[9]). Furthermore, when the accuracy of the calibrated absolute displacement was verified based on the data[9] gathered at the Chouyo, Takamori, Kumamoto, Kumamoto-Oguni and Kikuchi stations, the horizontal error (standard deviation) was 19.3 cm and the vertical error (standard deviation) was 5.8 cm. The former value of 19.3 cm in the horizontal direction is large, but considering that the interferometry SAR is the average value of the displacement of 20 square meters of ground surface, while GNSS is a point, it seems to be a value that can occur in the event of a major disaster. Such deformation data[10)–12)] that were produced of the three-way components obtained in this way (Shimada, 1999, Shimada et al., 2017 and Shimada, 2018) were used in this paper. The three-component displacements were indicated as mesh data at 12.5 m intervals. The SAR data used for the analysis were in total six images: the southbound right observation on March 7 and April 18, the northbound left observation on April 15 and 29, and the southbound left observation on April 15 and 29. Results showed that the entire Aso Valley, including the somma on the north side, displayed several tens of cm of displacement to the north. Fluctuations were observed, but there are places where the amount of fluctuation is particularly large in the Uchinomaki district within a diameter of about 1 km, in the Kario district and the Matoshi district.

Based on this data, the survey lines were selected as perpendicular to the grabens in the Ozato, Uchinomaki, Kario and Matoishi districts as shown in Fig. 9, and horizontal displacement, vertical displacement and horizontal strain along them were calculated and drawn as shown in Figs. 10 to 13. The three-component separation data obtained from this S AR analysis is expressed for each 12.5 m mesh in the east-west and north-south directions. Then, secondary meshes were formed at regular intervals along the defined survey lines, and the three components were calculated by interpolation from the surrounding four-point data. Furthermore, the components in the direction of the survey lines were obtained by coordinate rotation. After that, the horizontal strain was calculated by dividing the amount of displacement between two adjacent points by the distance between the two points.

The data are plotted at regular intervals along the survey lines. The intervals vary depending on the orientation and are 20 to 30 m in this analysis. The horizontal displacement toward the left side (north

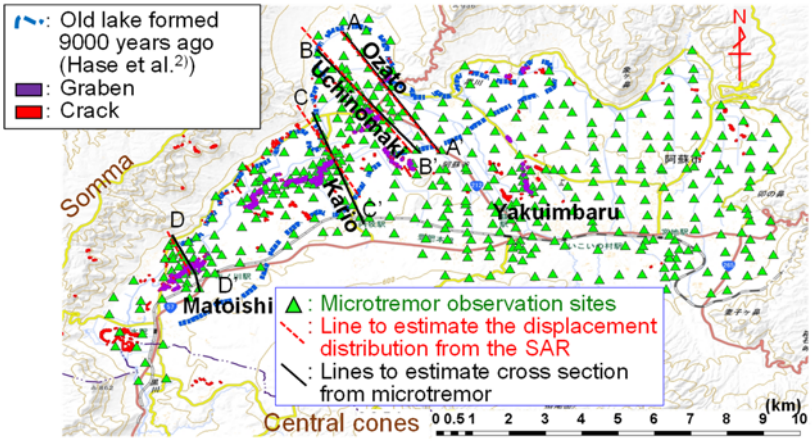

Fig. 9 Microtremor sites and studied survey lines

side) is indicated by "+" in all figures, since local horizontal displacement occurs from the southeast to the northwest. In addition, as described above, horizontal displacement occurred in the entire Aso Valley, and in order to distinguish the local displacement amount, the estimated displacement caused throughout Aso Valley is shown in the blue one-dot chain line in the horizontal displacement distribution map of each figure. The southeastern end of each survey line is a point where there is no local displacement (excluding the Matoishi district because it is larger than other areas), and the northwestern ends of the Kario and Matoishi districts are the somma. As the average displacement at these points was 42 cm, this was regarded as the displacement throughout Aso Valley. In addition, the locations where grabens and cracks occurred are indicated by broken lines in the figures. The characteristics of each district are as follows. Note: the ground surface slope that rises toward the northwest (the starting point of the distance marker) is indicated as "+".

(1) Ozato district: The ground surface gradient is almost flat at −0.1% from point **p** to point **r** on the southeast side of the Kuro River, and slightly drops to about −0.9% northwest from the graben section to the vicinity of the Kabaru River. The lowest point is near point **t**, which crosses the Kabaru River, then 0.1% to point **u**, and then 0.5%, gradually increasing northwest. The local horizontal displacement gradually increases to about 50 cm from the vicinity of point **q** to the graben section, and once it decreases, a large displacement of 1.3 m appears on the northwest side in the graben section. It gradually becomes smaller and becomes zero near the point **u**, and a small displacement toward the southeast occurred on the somma side. On the other hand, the vertical displacement gradually rises to the northwest side from the vicinity of point **q**, drops sharply in the graben section, and then gradually rises to the vicinity of point **v**. A large tensile strain of −2% is generated in the graben section, and a small compressive strain is generated near point **u** to point **v**.

Therefore, it is considered that the range from point **q** to point **u** was displaced to the northwest side, and point **s** was further displaced, resulting in a large tensile strain there. In addition, since the range from point **A** to point **v** was slightly displaced to the southeast, it is probable that the horizontal movements collided with each other and swelled near point **v**, which was between the two ranges, causing compressive strain.

(2) Uchinomaki district: The surface gradient drops slightly northwest from **B'** at the southeastern end to the vicinity of point **r** in the graben section at about −0.4%. Then the ground surface is almost flat to point **t**, which crosses the Kabaru River through the hot spring town at about −0.2%. After that, it rises a little at 0.6% up to the vicinity of the Yunoura River, and after crossing the river, it rises at about 3.1% toward somma. Local horizontal displacement occurs in a wide range in the northwest direction from point **p** to point **u**, and then a small displacement in the southeast direction of about 0.3 m occurs in the vicinity of **B**. A large displacement of about 1.6 m occurs near point **s,** where a graben occurred, and a displacement of more than 1 m occurs in the hot spring town to the Kabaru River, but the distribution is complicated. The vertical displacement rises a little between points **q** and **u**, but even within that range, it subsides locally in the two graben sections. Tensile strain is generated in the graben sections.

Therefore, it is considered that the entire range from point **p** to the vicinity of point **u** was displaced to the northwest, and the vicinity of point **s** was further displaced and a large tensile strain was generated. In addition, since the range from **B** to point **u** was slightly displaced to the southeast, it is considered that they collided with each other near point **u** in the middle of the two ranges and swelled a little, causing compressive strain.

A seismograph by Kumamoto Prefecture is installed at the Uchinomaki branch in Aso City at point **m** in (a), and records have been taken at the time of the main shock[13]. In the acceleration waveform of the NS component, a spike-like peculiar behavior appears around 20 seconds. When the displacement waveform is estimated by integrating this waveform, a maximum displacement of about 3.5 m occurred in the north direction after 20 seconds, and a residual displacement of about 2.5 m occurred after 60 seconds [14]. According to the measurement by SAR, the displacement amount was about 2 m, and the two are in good agreement.

(3) Kario district: The ground surface gradient drops slightly northwest from **C'** at the southeastern end to the vicinity of point **r** in the graben section, at −0.8%, and from there to the Kuro River, it is almost flat at about −0.2%. There is a long and narrow ridge from somma to the northwest of the Kuro River, which is complicated, but the survey line hits the ridge near point **y**. In the range from the Kuro River

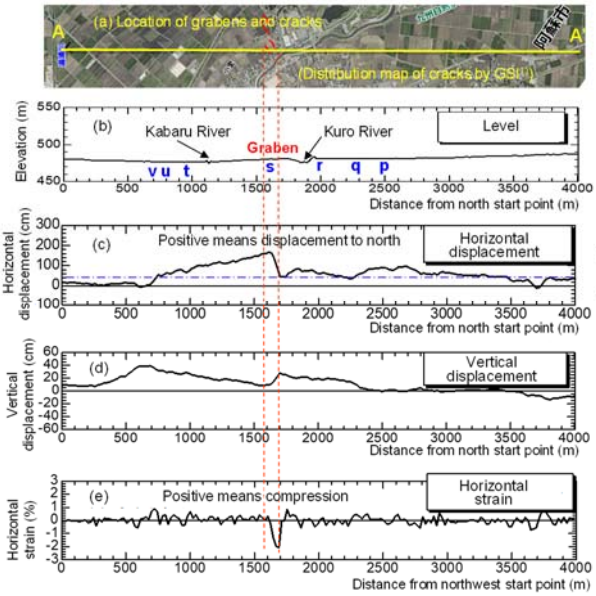

Fig. 10 Distribution of displacement and strain in the Ozato district

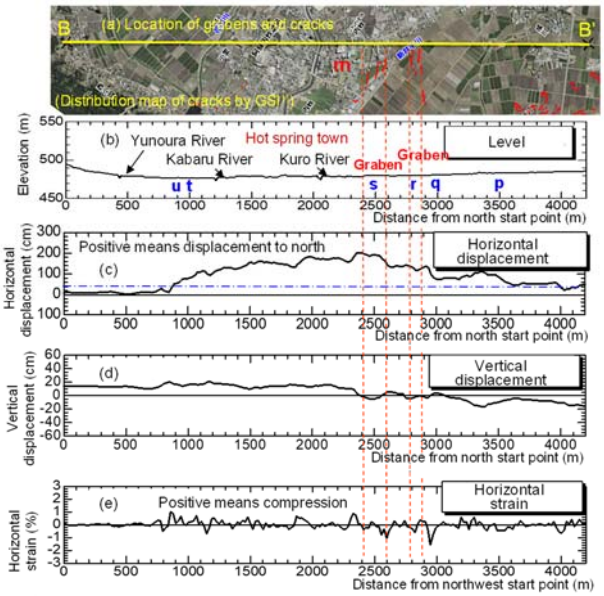

Fig. 11 Distribution of displacement and strain in the Uchinomaki district

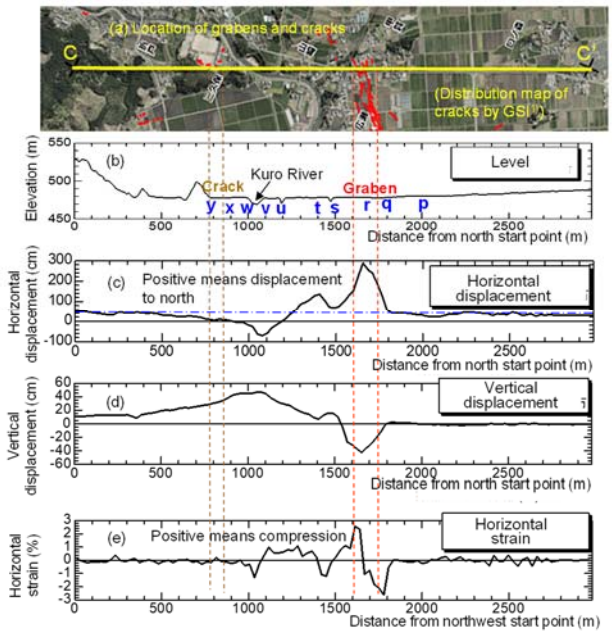

Fig. 12 Distribution of displacement and strain in the Kario district

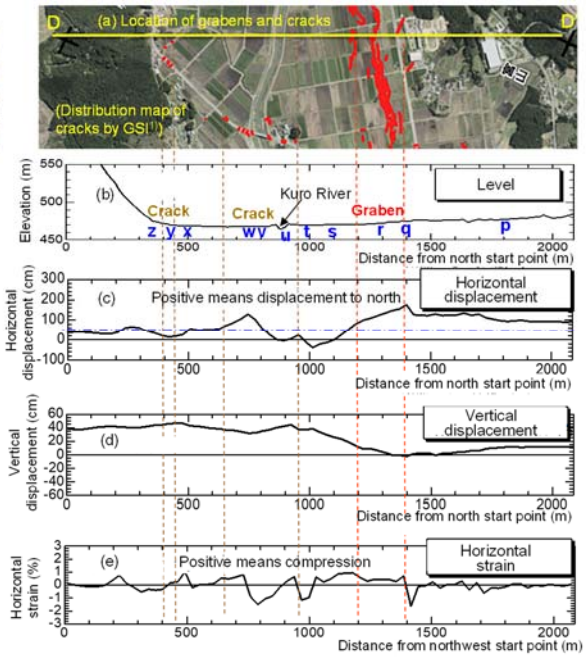

Fig. 13 Distribution of displacement and strain in the Matoishi district

to point **y**, the gradient increases slightly to about 0.4%. The local horizontal displacement is zero from **C'** to point **q**, and a large displacement begins to occur suddenly in the northwest direction from there, reaching a maximum of 2.5 m at point **r**. After that, it decreases to the vicinity of point **s**, then increases again near point **t**, and decreases to zero near point **u**. On the northwest side of that, there is a displacement toward the southeast. The distribution of vertical displacement is axisymmetric to the distribution of horizontal displacement, and it subsides significantly in the graben section and rises up to about 55 cm around point **w**.

Therefore, it is considered that the range from point **q** to the vicinity of point **u** was displaced to the northwest, and the vicinity of point **r** was further displaced, resulting in a large tensile strain there. In addition, since the area near point **v** to point **y** was slightly displaced to the southeast, it is probable that the horizontal movements of both collided and swelled near point **t** to point **x** in the middle of the two

ranges. A crack has occurred near point **y**, which is the boundary with the somma. Although the displacement was small, it extended toward the southeast, so it is probable that a tensile crack occurred. In addition, cracks also occurred in the lower left of the crack distribution map in (a) in Fig. 12. Moreover, many cracks occurred along the edge of somma on the southwest side in Figs. 1 and 5. It is probable that these cracks were also caused by tensile force.

(4) Matoishi district: The ground surface gradient drops by −1.4% northwest from the southeastern end **D'** to the vicinity of point **q**, and suddenly drops to about −2.7% between the points **q** and **r**, where a graben occurred. From there to the Kuro River, it descends with a gentle gradient of about −0.8%. After crossing the Kuro River, it rises a little to the vicinity of point **y** at about 0.6%, and from there it climbs to point **z** at the foot of the somma at about 5%. The local horizontal displacement is zero from D' to point **p**, and a slight northwestward displacement begins to occur from there, reaching a maximum of 1.3 m near point **q** in the graben section. After that, the amount of displacement gradually decreases, and after a displacement in the opposite direction occurs from the middle to the vicinity of the Kuro River, a displacement in the northwest direction occurs again from the vicinity of point **v**, and the displacement becomes about 1 m near point **w**, then decreases. The distribution of vertical displacement tends to subside near points **q** and **w**, where the horizontal displacement is large, and conversely, it rises a little near points **t** and **y**. The strain has a complicated distribution, and tensile strain occurs near points **q** and **v**.

Therefore, it is considered that the range from point **p** to point **s** was displaced to the northwest, and point **q** was further displaced, resulting in a large tensile strain there. In addition, since the range near point **t** to point **w** was slightly displaced to the southeast, it is considered that the horizontal movements collided with each other near point **t** to point **u** in the middle of the two ranges and generated swelling. The area around point **w** to point **x** moved to the northwest, and the range from point **x** to point **y** moved in the opposite direction. Therefore, it is considered that a tensile crack occurred near point **y**. The Taisho Bridge is located 400 m southwest of this survey line. Here, the embankment road on the left bank was pushed toward the river, which is thought to be due to the compressive strain seen near point **u**.

The authors also examined the graben in the Yakuimbaru district, but since it became clear that the mechanism of occurrence was different, the outline of the examination results is shown separately in Appendix 1.

4. STUDY ON GROUND FORMATION, CHARACTERISTICS, AND DEFORMATION DURING PAST EARTHQUAKES IN THE ASO VALLEY

4.1 Investigation on the sedimentation process after the formation of the caldera

It is presumed that old lakes have been formed in the Aso Caldera at three different times in the past. According to Hase et al.[2)], it is estimated that there were no lakes or rivers flowing in the Aso Valley 21,000 years ago in the latter half of the last glacial period. After that, volcanic activity occurred in the western part of this area, and rivers were blocked by the outflow of lava, forming the newest lake. As shown in Fig. 1, it is estimated that a large lake existed in the southwestern part of the Aso Valley around 9,000 years ago. The lake remained stable to about 8,800 years ago, after which its water level gradually dropped and it shrank due to sedimentation and erosion of the drainage section (near Tateno barranco), and eventually a river basin was formed. Borings taken in the Uchinomaki and Kario districts show that a gravel layer of river formation appeared about 21,000 years ago at an altitude of about 400 m, a thick clay or silt layer formed on the upper part of the lake, and silt or sand was further deposited on the surface layer. The layer referred to later as the lake deposit in this paper corresponds to the clay or silt layer above the river gravel layer.

To understand the distribution of this lake deposit and the sand or clay layer above it in the area where grabens occurred, existing boring data were collected. When the authors first checked the Geo-informatic Sharing Database in Kyushu, there were only 126 boring data from the target area. Since these were not enough, the authors collected data from the Kyushu Regional Development Bureau of the Ministry of Land, Infrastructure, Transport and Tourism, Kumamoto Prefecture, Aso City, Kyushu

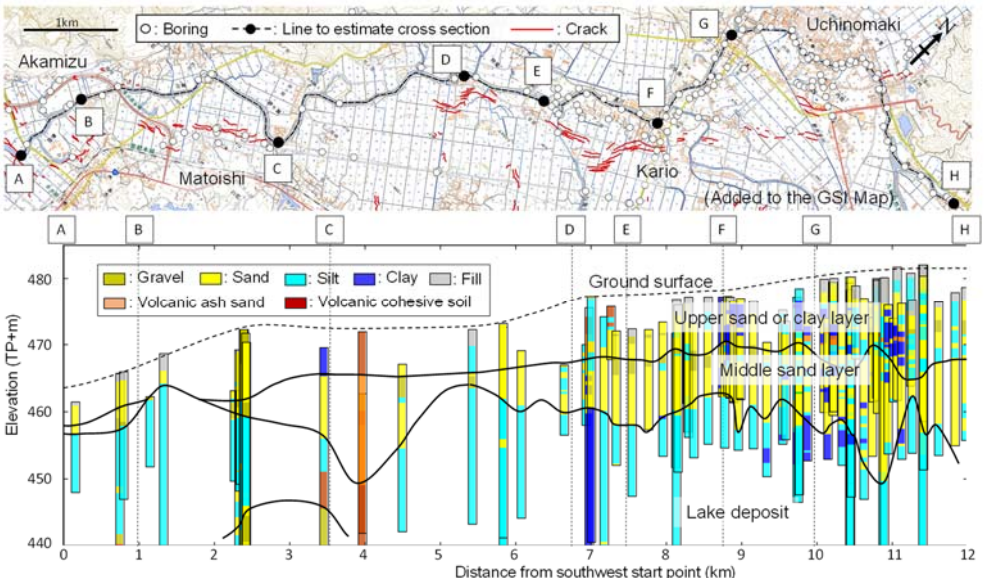

Fig. 14 Soil cross section along the Kuro River estimated from existing boring data

Electric Power Co., Inc., and private organizations. As a result, they added 468 data from Kumamoto Prefecture, 132 data from Aso City, and 41 data from the private sector. Figure 14 shows the soil cross section along the Kuro River from the Akamizu district to the Uchinomaki district estimated from these data. The stratification is divided into three layers: an upper sand or clay layer, a middle sand layer, and the lake deposit, which is mainly composed of soft clayey soil. The upper surface of the lake deposit fluctuates at an altitude of around 460 m throughout the target area. Since few of the previous boring surveys have been investigated deeply, the lower surface of the lake deposit cannot be estimated accurately. The upper sand or clay layers deposited on the surface are uniformly distributed with a thickness of about 10 m. These layers are considered to be river sediment that has been deposited since the lake shrank to become a river basin. The rapid change from lake stratification to river sediments suggests that the lake, which was relatively deep, had rapidly become shallow due to the opening of the drainage section by fault movement or due to rapid sedimentation[15]. The middle sand layer is partially deposited along this survey line. This layer may contain debris flow deposits from somma and riverbed gravel of the Kuro River. In the section from G to H in Uchinomaki, hot spring water may rise from underground and become hard due to silicification. This can be seen in the microtremor array observation results, which will be described later.

4.2 Investigation of similar ground deformation caused by past earthquakes

Since it is important to elucidate the mechanism of the grabens whether or not similar grabens occurred during past earthquakes, the authors interviewed the Aso City Government and surveyed the relevant literature. As a result, similar damage was found at an archaeological site, described in Appendix 2.

5. DETAILED INVESTIGATION OF GEOTECHNICAL CHARACTERISTICS IN A TYPICAL DISTRICT

5.1 Survey of soil profile in the Kario district by boring, etc.

A detailed soil investigation is required to clarify the mechanism of local ground deformation. Therefore, of the four districts, the Kario district, which suffered the most severe damage to housing, was investigated. First, the collected boring data were examined, but most of the past borings were shallower than 20 m, too shallow to determine a soil profile. Thus, borings were conducted at four sites along

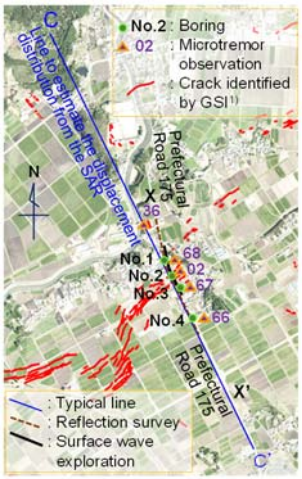

Fig. 15 Sites of soil investigations and explorations

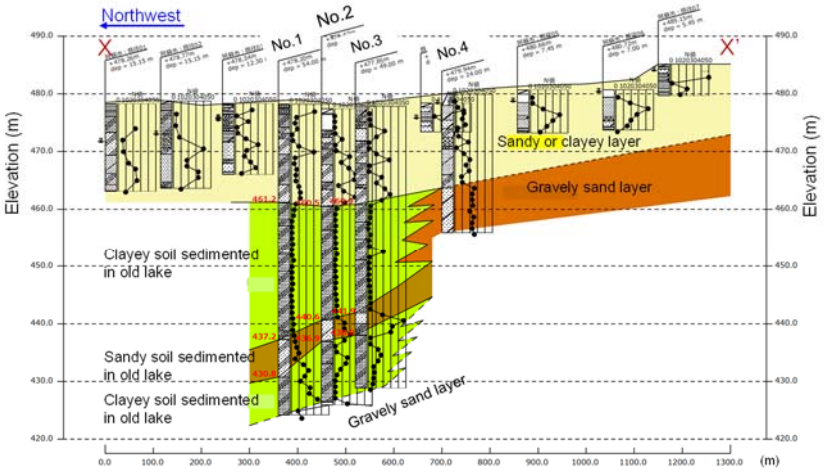

Fig. 16 Soil cross section in the Kario district

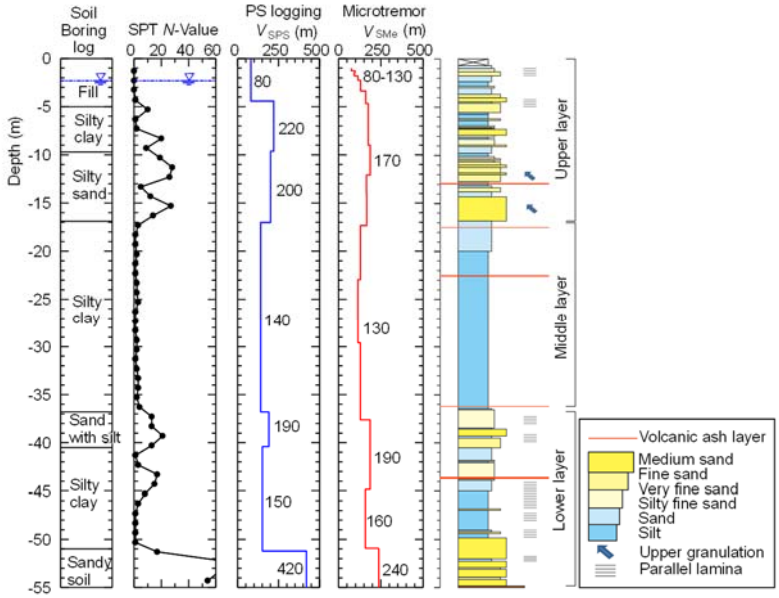

Fig. 17 Results of soil boring log, PS logging, microtremor array measurement and core observation at the No.2 site

Prefectural Road 175: the northwest side (No. 1), the graben point (No. 2), the southeast side (No. 3), and a further south side (No. 4), as shown in Fig. 15. Based on these borings, the soil cross section along about 1,300 m of the road in the section from X (Mikubo) to X' (Otohime) was estimated, as shown in Fig. 16. Unconsolidated sand or clay is deposited at an altitude of from 478 m to 461 m with a thickness of about 17 m. The soil condition on the north side differs from the condition on the south side. Sandy soil and clayey soil are unevenly deposited from point X to around 800 m. Since the surface layer at No. 2 was cracked by the earthquake, looking at the soil boring log of No. 1, the SPT N value of the clayey soil is 4 to 7, which means a little soft, though there is a thin, very soft layer with $N = 1$ to 2. The N value of the sandy soil is about 10 to 30, which means medium dense. On the contrary, hard sandy soil with an N value of 15 to 40 is deposited on the southeastern side from around 800 m to point X'.

Under the unconsolidated soil layer, lake deposit is distributed on the northwest side and an alluvial fan of gravelly sand is distributed on the southeast side at a distance of 600 to 700 m. The soil composition of the lake deposit is clayey silt to silty clay, and the SPT N value is as small as 1 to 2 for the entire layer, though it is slightly larger near the layer boundary. In the lake deposit, a thin sandy soil

layer mainly composed of fine sand with SPT N value of 13 to 20 was interposed at an altitude of 440 to 430 m, and this layer contained a large amount of confined water. The elevation of the bottom of the lake deposit is 424 m at No. 1, 426 m at No. 2, and 429 m at No. 3, and it gradually becomes shallower toward the southeastern side. Since there is no lake deposit at No. 4, it is presumed that the bottom of the old lake is steep. The groundwater level at No. 2 is GL −2.3 m.

The No. 2 boring point is located in a graben and is about 1.7 m lower than both sides. Therefore, if this difference is taken into consideration and the three boring results of Nos. 1 to 3 are compared in the horizontal direction, it should be possible to know how deep the subsidence extends. However, since the unconsolidated soil layer was not homogeneous, the depth of subsidence could not be determined. On the other hand, the elevations of the upper surface of the lake deposit were 461.2 m, 460.5 m, and 460.9 m in the order of No. 1 to 3. Although the No. 2 point was slightly lower, there was no difference as large as the step on the ground surface. Therefore, it is considered that subsidence occurred mainly in the unconsolidated soil layer.

PS logging was also performed at boring point No. 2 in the graben. The depth distribution of the S wave velocity is shown in Fig. 17. V_S is slow at 80 m/s, probably because cracks occurred up to GL −4.4 m, but the unconsolidated soil layer up to GL −17 m below it is V_S = 200 to 220 m/s. In the lake deposit below, the clayey soil to the bottom of GL −51.2 m is a little slow with V_S = 140 to 150 m/s, and the sandy soil in the middle is 190 m/s. In the sandy soil under the lake deposit, V_S = 420 m/s, which is fast.

At this point, other holes were also dug to take a boring core and soil samples with less turbulence. The results of observing the boring core at site No. 2 are shown in Fig. 17. This core was composed entirely of silt to medium sand. The unconsolidated soil layer up to GL −17 m on the surface was mainly composed of sandy silt to fine sand, and the grain size changes drastically with depth. This layer contains a lot of fine gravel and some pumice gravel. There are many pyroclastic materials, such as scoria glass, among the soil particles. Coarse grains are deposited on the bottom, and fine grains are deposited on the top, so this layer is considered to be a river flood deposit. The lake deposit up to GL −36 m is silt, and most of the upper part of the layer is of grayish white volcanic ash origin. The lower part is bluish gray and relatively homogeneous. Since diatoms are contained, it is presumed that this layer was deposited in a freshwater lake. The lower layer is composed of sand, silt, and sand. Below GL −54.8 m, it changes to a gravel layer. This gravel layer is the basal layer of the lake. The water content of the core silt layer at GL −42 to −43 m was very high.

5.2 Investigation of soil characteristics by laboratory tests

Soil samples with less turbulence were taken at the No.2 site using thin-wall tube samplers for clayey soil and triple-tube samplers for sandy soil. Then, laboratory tests were conducted to determine the density, water content, particle size, liquid/plastic limit, shear strength, consolidation, cyclic deformation, and cyclic undrained shear strength of the soil samples. Figure 18 shows the depth distribution of the natural water content, the liquid limit and the plastic limit. This figure also includes the results of tests conducted in the past geotechnical investigation by the Aso City Government. From the ground surface to around 460 m above sea level, there is an upper unconsolidated soil layer with a natural water content of around 100%. On the other hand, the clayey soil of the lake deposit at an altitude of 460 to 440 m has a very high natural water content of 200 to 300%. The liquid limit is 150 to 230%, and the natural water content is higher. For example, the water content of the sample collected from a depth of 26.4 m was 278% and the void ratio was 7.0, which were abnormally large. However, according to the triaxial compression test (UU), c = 68 kN/m^2, $\varphi = 0°$, and the strain at failure was 1.5 to 1.9%, which means a comparatively hard, cohesive soil. Even so, once it was remolded, it became muddy and the specimen could not be prepared again. It was a sensitive cohesive soil classified as silt with a high liquid limit.

Next, in order to perform seismic response analysis and residual deformation analysis, two types of tests were performed on the unique clayey soil of the lake deposit using a cyclic torsional shear test apparatus. Since the seismic response analysis was performed using the FLUSH computer program, a normal cyclic deformation properties test was performed. Figure 19 shows the results of this test on clayey soil taken from two depths of the lake deposit. The shear modulus ratio G/G_0 at a shear strain of 10^{-3} was about 0.8, which was slightly larger than the shear modulus ratio of ordinary cohesive soil.

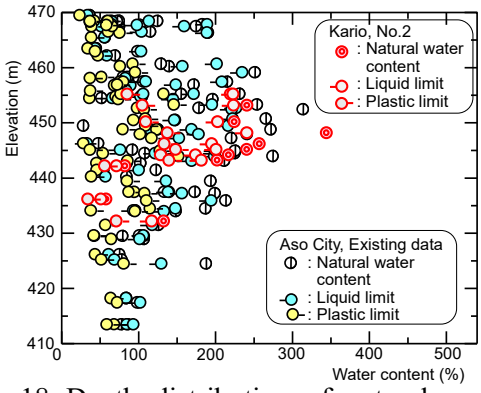

Fig.18 Depth distribution of natural water content, liquid limit and plastic limit

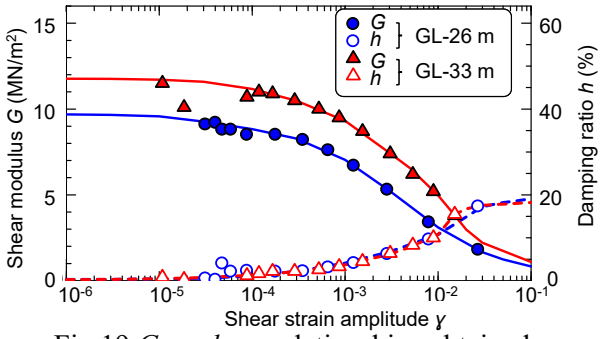

Fig.19 G - γ, h - γ relationships obtained by cyclic torsional test

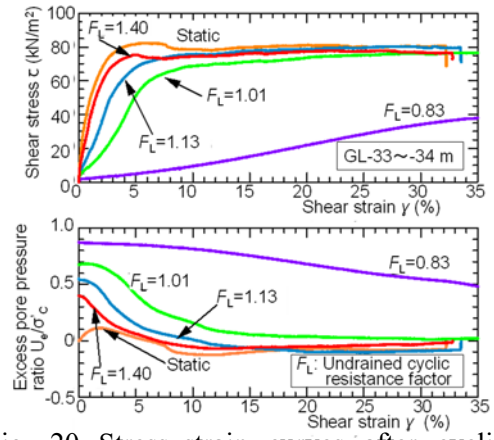

Fig. 20 Stress–strain curves after cyclic loading in different F_L

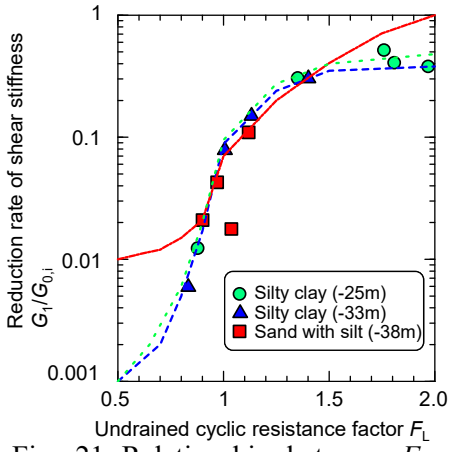

Fig. 21 Relationship between F_L and $G_1/G_{0,i}$

Since the residual deformation analysis was performed using the ALID computer program[16], the samples were taken at depths of 25.0 to 26.85 m and 33.0 to 34.0 m for the clayey soil and 38.5 to 40.4 m for the sandy soil. The test was carried out by the same method as the test for liquefaction of sandy soil and subsequent deformation characteristics. As a result, the liquefaction strength (cyclic undrained shear strength ratio) R_L (N_L = 20, γ_{DA} = 7.5%) was 0.889, 0.542, and 0.352 at the three depths, respectively. In the monotonic loading test after cyclic loading, the shear strain – shear stress and shear strain – excess pore pressure ratio relationships were obtained. Test results at a depth of 33.0 to 34.0 m are shown in Fig. 20. Here, F_L is the undrained cyclic resistance factor, which has the same meaning as the safety factor for liquefaction, and is the value obtained by dividing R_L by the cyclic shear stress ratio applied to the specimen. As can be seen in this figure, when a cyclic shear stress exceeding R_L is applied (that is, F_L<1), the shear stiffness decreases sharply. Based on these data, the relationship between F_L and shear modulus ratio were plotted in Fig. 21, where, G_{0i} is the secant modulus when the shear strain is 10^{-3} in the test without cyclic loading, indicated as "static" in Fig. 20. The shear stiffness decreases to about 1/100 when F_L falls below 1 for all three depth samples. Therefore, it was found that this soil, even though it is clayey, has properties similar to those of liquefied loose sandy soil.

As mentioned above, the authors have focused on unique characteristics of the lake deposit and conducted in-situ and laboratory tests. The SPT N value of this clayey soil is very small, 1 to 2, and estimating the cohesion c from the empirical formula $c = 6.25N$, c is about 6 to 12 kN/m^2, which is significantly smaller than the result of the triaxial compression test. Therefore, although it is usually a fairly hard silt, it has the same characteristics as collapsible soil whose shear strength and shear stiffness drop sharply due to the impacts of standard penetration tests or strong shaking during earthquakes. This is apparently due to the large water content and void ratio, but, in essence, it is a special lake deposit in which pyroclastic materials containing pumice were deposited where diatoms were growing in the lake.

In other words, (1) the chain-like structure with large voids formed between diatoms was broken by strong shaking, and (2) pumice was porous and weakened by weathering for many years, and the particles themselves were broken by strong shaking.

The loosely deposited sand breaks the particle structure due to strong shaking and liquefaction occurs as it occurred in the 1964 Niigata Earthquake et al.[17]. The weathered pumice layer is destroyed by strong shaking and flows as occurred in the 1984 Naganoken-seibu Earthquake[18]. In addition, quick clay in which sodium ions were leached from marine clay distributed in Northern Europe collapses and flows due to impacts, as occurred in Lisa, Norway in 1978[19]. It seems that the lake deposit in Aso is a little different from these clays, but future research, such as detailed observation of the particle structure, is considered necessary.

5.3 Survey of a wide range of soil profiles by geophysical explorations

In order to investigate the soil profile not only at the boring site but also over a wide area around it, surface wave exploration was performed on the shallow layer, and reflection method exploration and microtremor array observation were performed on the deep layer. Appendix 3 shows the details of the equipment used for these explorations, the observation methods, and the data processing methods. Surface wave exploration was conducted from July 31 to August 3, 2017 in the three residential districts of Kario, Uchinomaki, and Ozato. In the Kario district, surface wave exploration was carried out on a 300 m survey line with a graben in between, as shown in Fig.15. In the measurement, 24 receivers were arranged in a straight line every 2 m to form one unit. As shown in Fig. 22, the S-wave velocity of the unconsolidated soil was slightly slower in the graben section than on both sides, and there was a clear difference, especially from the southeastern side. Similarly, the S wave velocity in the graben section decreased in the Uchinomaki and Ozato districts. As mentioned above, in the Kario district, the ground moved to the northwest by about 2.5 m near the graben section, and it is considered that a large tensile strain of about 2.5% occurred. Therefore, as shown in Fig. 23, it is considered that the horizontal earth pressure decreased and subsidence occurred as if the unconsolidated soil dropped.

In order to investigate how the depth of the cracks that occurred during the earthquake changed after the quake, Swedish weight soundings were conducted in the Kario district two years after the earthquake. As a result, it was found that the cracks were generally in the range of 0.3 to 2.0 m from the ground surface. However, cracks remained to a depth of 3 m or 5 m in some places.

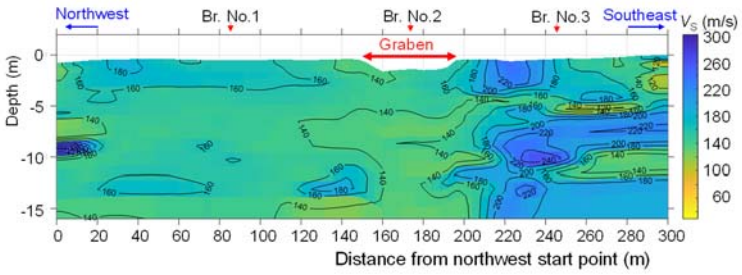

Fig. 22 Distribution of S-wave velocity measured by surface wave exploration in the Kario district

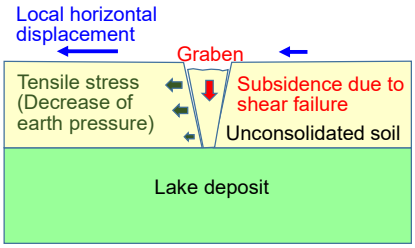

Fig. 23 Process of graben occurrence

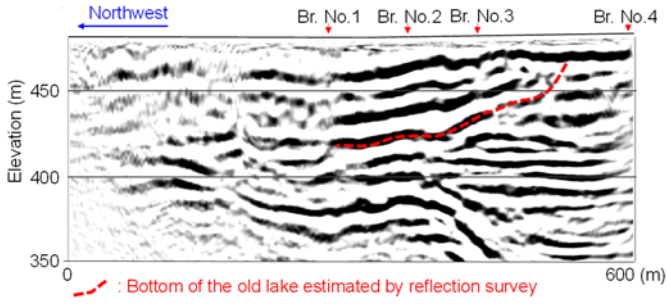

Fig. 24 Results of reflection tests conducted in the Kario district

A reflection survey was conducted from July 7 to 8, 2018 with the same survey line as shown in Fig. 15. In this exploration, the receiving point interval was 5 m, the oscillation point interval was 2.5 m, and the movement interval was 115 m. The length of the survey line was 600 m, and the number of receiving points and oscillation points was 125 and 257, respectively. As shown in Fig. 24, the red line in the figure is judged to be the bottom surface of the lake deposit, but unfortunately it is not clear on the northwest side from Br. No.1.

Microtremor array observations were first performed in and around the area where grabens occurred among the observation sites shown in Fig. 9. The numbers of locations and observation dates were 9 on May 20 to 22, 2017, 30 on June 12 to 13, 2017, 27 on July 31 to August 2, 2017, 92 on August 20 to 24, 2018, and 62 on August 29 to 30, 2019. The seismometer used was an integrated microtremor observation device (JU410), and observations were made at each point for 15 minutes. The observation results were analyzed and the depth distribution of the S wave velocity up to a depth of several tens of meters was estimated. In Kario district, observations were made at five locations along the survey line as shown in Fig. 15. The shear wave velocity Vs at Br. No. 2 estimated from microtremor array observation is shown in Fig. 17 in comparison with the shear wave velocity estimated from PS logging. From the surface layer to the bottom of the lake deposit near GL −51.2 m, both Vs showed fairly good agreement and were as low as 140 to 160 m/s. On the other hand, in the lower sandy soil layer, the V_S of both were large, 420 m/s in the PS logging and 240 m/s in the microtremor array observation. Both values differ in this layer, but the purpose of boring at this location is to confirm the bottom of the old lake, and only 4 m from the bottom was dug. Therefore, the reliability of V_S of the sandy soil layer measured by PS logging must be low due to the short measurement range. PS logging is also being carried out at KiK-net Aso (KMMH04)[20], which is about 2 km west, and the sedimentation environment there is similar to that of Br. No.2. The V_S of the sandy soil there is 280 m/s, which is close to the V_S measured by microtremor at Br. No.2. In addition, since this layer is sandy soil, rather than rock, V_S from microtremor was considered to be more correct. The lake deposit has some sandy soil layers in between, but the Vs is about 150 m/s as a whole. Therefore, the authors decided to consider the depth of Vs above 200 m/s as the bottom of the old lake by choosing the median of the two values. Then, by adding the results of other microtremor array observations along the survey line, it was estimated that the bottom of the old lake is bowl-shaped, as shown in Fig. 25.

In this cross section, the slope of the bottom of the old lake is gentler on the northwest than on the southeast. In the survey lines of all four districts, including the Kario district, there is somma on the northwest side, and in the Ozato, Uchinomaki, and Matoishi districts, the slope of the bottom of the old lake is steeper on the northwest of the somma side. There should be a similar tendency in the Kario district. However, as shown in Figs. 5 and 9, the line to estimate displacement distribution from SAR is taken toward the elongated ridge from somma, so, the bottom of the old lake should rise sharply. On the contrary, since the reflection survey and microtremor observations were carried out along Prefectural Road 175, the survey line of the cross section shown in Fig. 25 is along the Road 175. This survey line is the same as the survey line for SAR from Br. No.4 to Br. No.1, but the two survey lines separate from Br. No.1 because Road 175 turns eastward to avoid the elongated ridge, as shown in Fig. 15. Therefore, the slope of the bottom of the old lake on the northwest side of Fig. 25 has a gentle slope.

6. REPRODUCTION OF THE GRABEN BY SEISMIC RESPONSE ANALYSIS AND RESIDUAL DEFORMATION ANALYSIS

6.1 Analysis in the Kario district

In order to try to reproduce the graben in the Kario district by analysis and examine the mechanism, seismic response analysis was first performed using FLUSH on the cross section of Fig. 25. Seismic waves were recorded by the National Research Institute for Earth Science and Disaster Resilience (NIED) in 2016 on the ground surface of K-NET Ichinomiya (KMM04)[20], where no ground deformation occurred in the Aso Valley at the time of the main shock of the Kumamoto Earthquake. Therefore, one-dimensional seismic response analysis (DYNEQ) was performed, and the seismic waves generated at

the base were estimated, as shown in Fig. 26, and used as the input seismic waves for FLUSH in the Kario district, because no seismic record was observed there. The ground model for DYNEQ was set based on the soil boring log and the V_S measured at K-NET Ichinomiya. However, while a peak acceleration of 350 cm/s^2 was recorded at K-NET Ichinomiya, it was estimated that about 400 cm/s^2 was generated in Kario. This is because Kario is a sand or clay ground, while K-NET Ichinomiya is a gravel ground and Kario is closer to the epicenter. Therefore, the authors decided to use the analyzed result by gradually changing the amplitude of the wave input to FLUSH, with respect to the cross section of Kario district so that it would be about 400 cm/s^2 on the ground surface. Next, the maximum horizontal shear stress of each element was obtained from the analysis using FLUSH, and the F_L of each element was calculated. Then, the amount of decrease in shear modulus of each element was evaluated from Fig. 21, and the amount of residual deformation was calculated by residual deformation analysis (ALID[16]).

Figure 27 shows the velocity response spectrum (h = 5%) of each component from the record at K-NET Ichinomiya (KMM04). From this, it can be seen that both the east-west and north-south components peak near a period of 3 seconds. In addition, peaks appear in the east-west component at a period of 0.3 seconds and around 1 second. As mentioned above, the lake deposit is thick in the Aso Caldera, and from the soil investigation data shown in Fig. 17, the natural period of the ground is estimated to be about 1.25 seconds using the formula of $T_G = 4\Sigma(V_{Si}/H_i)$. From this, it was considered that the east-west component of seismic motion was more responsive than the north-south component, so in this study, the east-west component of seismic motion was selected as the input seismic motion.

The soil parameters used in these analyzes were set as follows. The soil investigation showed that the ground water of the sandy layer in the lake deposit is confined, and as a result, it was judged that the effective overburden pressure of the lake deposit must be reduced by about 15 to 20%. Therefore, the R_L value was multiplied by 0.85 with the test value and used in the calculation of F_L. In addition, since there is no particularly loose sand in the unconsolidated soil layer on the surface and no liquefaction traces, such as sand boiling, were observed, it was presumed that the strength and deformation characteristics due to seismic force did not change. Furthermore, though the V_S of the north side of the unconsolidated soil layer differs from the V_S of the south side of the graben, as shown in Fig. 22, but sandy soil and clayey soil are unevenly deposited, including a locally hard layer called “Toga”, as shown in Fig.16, it was assumed to be a uniform layer in the analysis.

(1) Unconsolidated soil layer (assuming a uniform layer with a mixture of clay and sand): i) γ_t = 17.0 kN/m^3, ii) V_S = 200 m/s, iii) G/G_0 - γ & h - γ: relationship by Yasuda & Yamaguchi[21], iv) no reduction in shear modulus due to earthquake.

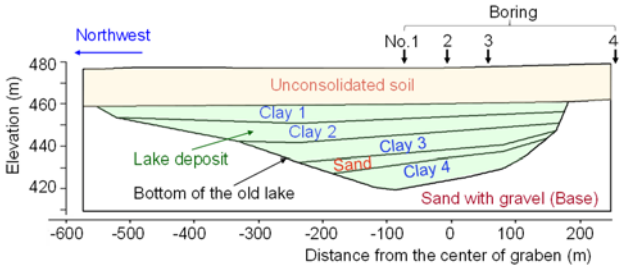

Fig. 25 Judged soil layer cross section in the Kario district

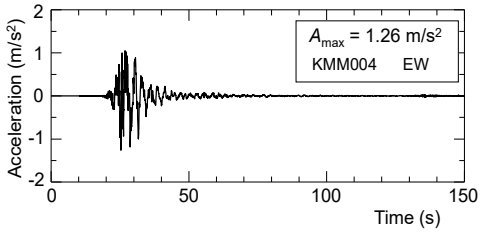

Fig. 26 Input seismic wave

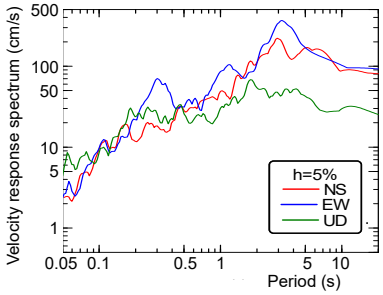

Fig. 27 Velocity response measured at K-NET Ichinomiya (KMM04)

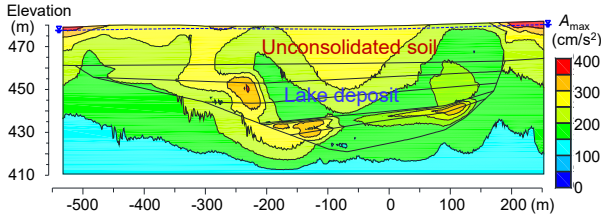

Fig. 28 Distribution of peak acceleration

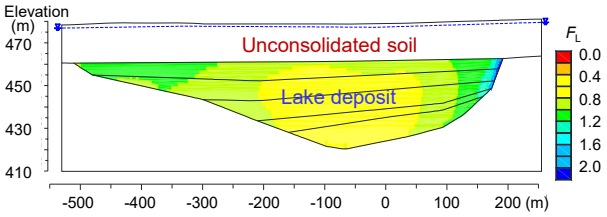

Fig. 29 Distribution of F_L

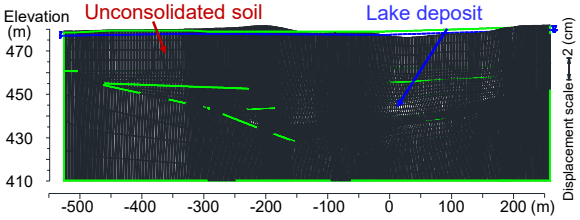

Fig. 30 Analyzed deformation (Lake deposit is divided into layers)

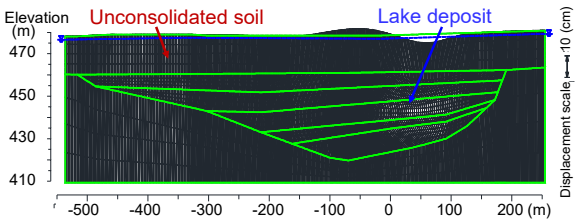

Fig. 31 Analyzed deformation (Lake deposit is assumed to be uniform)

(2) Lake deposit: i) γ_t = 12.0 kN/m^3 (Clay 1 to 3), 18.0 kN/m^3 (Sand), 14.0 kN/m^3 (Clay 4), ii) V_S = 140 m/s (Clay 1 to 3), 190 m/s (Sand), 150 m/s (Clay 4), iii) G/G_0 - γ & h - γ: test result, iv) R_L = 0.755 (Clay1 & 2), 0.460 (Clay 3 & 4), v) tested reduction in shear modulus (Fig. 21).
(3) Base: i) γ_t = 20.0 kN/m^3, ii) V_S = 300 m/s.

The distribution of the peak acceleration and F_L analyzed by FLUSH when the input seismic motion is adjusted to 1.25 times are shown in Figs. 28 and 29 (scale ratio X: Y = 3.5: 1), respectively. The point 0 m on the horizontal axis is the location where the graben occurred, and the left in the figure is northeast. The peak acceleration on the ground surface on both sides, where there is no lake deposit, is about 400 cm/s^2, but it is as small as 250 to 300 cm/s^2 in the central part on the old lake. In addition, the shape of the bottom of the old lake and the sand layer have a complex effect on the seismic response. The F_L in the central part of the bowl, which is the thickest layer of the lake deposit, is less than 1. Figure 30 shows the results of residual deformation analysis by ALID. The green line in the figure shows the ground model before the earthquake. Shear deformation occurs along the slope of the bottom surface of the lake due to the reduction of the shear stiffness of the lake deposit. Since the analysis is performed by the finite element method, it is not possible to reproduce the step shown in Photo 4, and the amount of displacement is smaller than the actual measurement. Even so, the ground surface subsided a little near the graben, and it swelled on the left side (northeast side). The distribution of such vertical displacement tends to be similar to the survey results from SAR, shown in Fig. 12, and it was considered that these analyses are likely to qualitatively reproduce the deformation.

6.2 Estimation of soil profiles and analyses to reproduce the deformation during the earthquake in other districts

As mentioned above, it was found from the microtremor array observation results in the Kario district that the boundary where Vs ≧ 200 m/s can be judged to be the bottom of the old lake. Then, microtremor array observations were added in the Ozato, Uchinomaki, and Matoishi districts to estimate the soil cross sections focusing on the depth and shape of the bottom of the old lake. Figure 9 shows all 401 sites of the microtremor array observation conducted in Aso Valley, including the sites conducted by the NIED[22]. Observation results at about 10 sites were arranged along the survey lines in the four districts, and spatial interpolation was performed between them to estimate the cross sections of V_S. In this estimation, first, the elevations of the survey lines passing through the microtremor array observation points were examined, and the shortest points from the array points to the survey lines (the foot of the perpendicular line from the array to the survey line) were set as the positions of the array in the cross sections. Next, the analyzed V_S was projected onto the survey line while maintaining the altitude of the array site. Finally,

spatial interpolation was performed using Generic Mapping Tools (GMT) and the surface spline method[23], which is the standard used for spatial interpolation of discrete data.

Then, the depth at which $V_S \geqq 200$ m/s was judged to be the bottom of the old lake, and seismic response analysis and residual deformation analysis were performed in the same manner as in the Kario district. The lines to estimate cross sections from the microtremor array observations were set to be close to the lines to estimate the displacement distribution from SAR, but there were some sections where the positions were slightly different due to the difference in the measurement points, as shown in Fig. 9. The input seismic wave of the seismic response analysis of each area is the same as that used for the analysis at the Kario district, but its amplitude was adjusted according to the fault distance. Fault distances at the center points of the survey lines of the Matoishi, Kario, Uchinomaki, and Ozato districts and at K-NET Ichinomiya, estimated based on the fault plane model set by the NIED[24], were 18 km, 22 km, 25 km, 25 km, and 30 km, respectively. Then, referring to the relationship between the fault distance and the peak acceleration proposed by the NIED[24], the amplitude of the input seismic wave was set to 1.25 times for the Matoishi and Kario districts and 1.15 times for the Uchinomaki and Ozato districts. The soil parameters were set as follows based on the values used in the Kario district. Since it was difficult to judge the sand layer interbedded in the lake deposits, observed in the boring core at Kario, from the tremor array observation, it was assumed that the lake-forming clayey soil layer has a uniform shear wave velocity. On the other hand, the unconsolidated soil layer was divided into three types according to V_S. Type 3 partially exists in the Uchinomaki and Ozato districts, with the former presumed to be silicified by hot spring water and the latter to be riverbed gravel. Since the ALID program uses FEM for analysis, though it is difficult to reproduce the step, the mechanism of the graben must be discussed based on the deformation of the analyzed result, the same as for the Kario district. If the surface soil layer is hard, the surface layer will not be easily deformed, even if the lake deposit is deformed. Therefore, the c and φ of types 1 and 2 were intentionally set to be slightly smaller, so that the surface layer is easily deformed as the lake deposit is deformed.

(1) Unconsolidated soil layer (clay or sand): i) divided into 3 types according to V_S of microtremor array observation (Type 1; $\gamma_t = 15.0$ kN/m^3, $V_S = 100$ m/s, $c = 0$, $\varphi = 10°$, Type 2; $\gamma_t = 17.0$ kN/m^3, $V_S = 150$ m/s, $c = 0$, $\varphi = 10°$, Type 3; $\gamma_t = 19.0$ kN/m^3, $V_S = 250$ m/s, $c = 0$, $\varphi = 35°$), ii) G/G_0 - γ & h - γ: relationship by Yasuda & Yamaguchi[21], iii) no reduction in shear modulus due to earthquake.

(2) Lake deposit (elevation of the upper surface is set to 460 m): i) $\gamma_t = 12.0$ kN/m^3, ii) $V_S = 140$ m/s, 100 m/s (only for Matoishi), iii) G/G_0 - γ & h - γ: tested result (Fig. 19), iv) $R_L = 0.460$, v) tested reduction in shear modulus (Fig. 21).

(3) Base: i) $\gamma_t = 20.0$ kN/m^3, ii) $V_S = 300$ m/s.

First, an analysis was conducted to confirm whether the same results as in Fig. 30 can be obtained if the lake deposit is assumed to be one homogeneous layer. The result is shown in Fig. 31, and since there is not much difference in deformation between the two, it was decided that analysis of the cross section estimated from the microtremor array observation could proceed. Figure 32 shows the estimated cross section from the microtremor array observation, the residual deformation analysis result, and comparison of the horizontal and vertical displacement distributions analyzed by ALID and measured by SAR. As mentioned above, the entire Aso Caldera moved northward by several tens of centimeters during the earthquake, so the horizontal displacements of the SAR are drawn by subtracting 42 cm. In the Ozato district, according to the SAR, the northwest side from around 2,300 m displaced northwestward, but on the contrary, it is displaced southeastward near the foot of somma, and the result is that it rises near the center. As mentioned above, the absolute displacement is smaller than the value actually generated, but the tendency of increase / decrease in horizontal and vertical displacement in the analyzed value was similar to the increase / decrease in actual measurement. Locally, the amount of horizontal displacement decreases once on the southeast side of the graben section and then suddenly increases on the northwest side. According to the cross section from the microtremor array observation, there is a layer with a relatively large V_S, which seems to be the riverbed gravel of the Kuro River, and it is considered that this may have influenced the displacement. The displacement distribution measured by SAR is complicated in the Uchinomaki district. According to the cross section from the microtremor

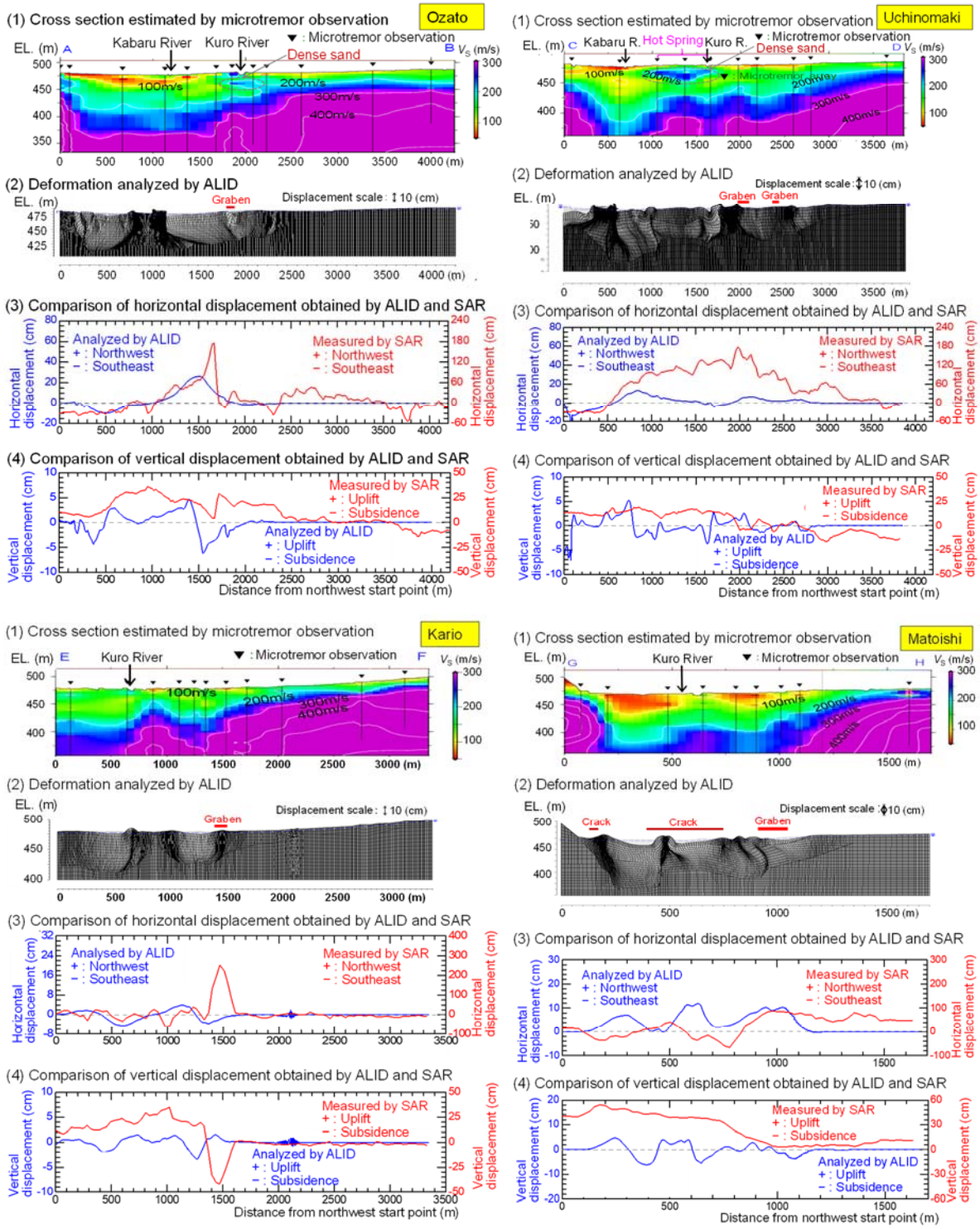

Fig. 32 Cross sections in four districts estimated by microtremor measurement and by analysis

array observation, the depth of the bottom of the old lake is intricate, and the surface layer of the Uchinomaki hot spring area contains a lens-like layer hardened by the silicification of hot spring water. Therefore, it is considered that the displacement distribution has become complicated. Residual deformation analysis also resulted in a complicated deformation. In the Kario district, as mentioned above, the northwest side from around 1,000 m is different from the survey line of the SAR. Therefore, when comparing only on the southeast side, the displacement distribution of the SAR showed a large

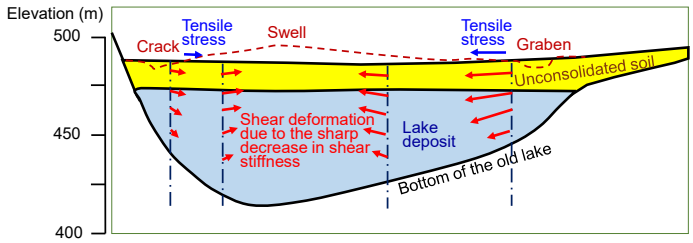

Fig.33 Mechanism of grabens

horizontal displacement in the northwest direction and subsidence in the graben section, and the analysis of the cross section from the microtremor array showed similar displacement and subsidence, though about 200 m deviated to the northwest. Since this area is a complex area with steep slopes at the bottom of the old lake, both deformations are considered to be fairly consistent, given the errors involved in the section estimation. According to SAR, in the Matoishi district, the horizontal displacement distribution from the graben section to the northwest side was first displaced to the northwest, then in the opposite direction before the Kuro River, and displaced to the northwest again. The horizontal displacement distribution of the analyzed result also tended to be close to these displacements.

As described above, the deformation obtained by the analysis conducted by combining the FLUSH and ALID programs for all four districts qualitatively matches the actual deformation. Based on these, the following conclusions were derived regarding the mechanism by which the graben occurred.

(1) A lake deposit of volcanic clayey soil containing diatoms and pumice and having a large void ratio is deposited in a lake that existed around 9000 years ago.
(2) The bottom of the old lake is bowl-shaped, as shown in Fig. 33, and the ground surface was also slightly inclined toward the center in some districts.
(3) The shear stiffness of the lake deposit decreased sharply due to the earthquake, resulting in shear deformation of the lake deposit so as to wrap around the central part.
(4) Due to this deformation, local displacement occurred in the surface layer near the edges on both sides of the old lake, and the surface unconsolidated soil layer was pulled horizontally, causing grabens and cracks. Also, in the central part, horizontal displacements from both sides collided and swelled.

7. CONCLUSIONS

In order to elucidate the mechanism of the grabens that occurred in various parts of Aso Valley due to the 2016 Kumamoto Earthquake, on-site reconnaissance, measurement of ground deformation, soil investigation, geophysical exploration, soil test and analysis were conducted. As a result, the following conclusions were obtained.

(1) The direction of the grabens is mainly from northeast to southwest, near the edge of an elongated old lake in the same direction that was estimated to have existed around 9,000 years ago. According to the displacement distribution of the ground surface measured by synthetic aperture radar (SAR), a horizontal displacement of 2 to 3 m occurred locally in the district where the grabens occurred. Then, when the displacement distribution of the survey lines from northwest to southeast in the orthogonal direction was taken, the horizontal displacement occurred from around the edges of the old lake on both sides toward the inside, and the vertical displacement was distributed so as to rise in the central part.
(2) The lake deposit is sediment as thick as 30 to 40 m, and river sediments (unconsolidated soil) are deposited on top of it to a thickness of 10 to 20 m. This lake deposit is a special clayey soil containing diatoms and pumice with a large void ratio, and has its shear stiffness decreases sharply due to cyclic shear stress, similar to the liquefaction of loose sand.
(3) Based on the soil investigation and the geophysical exploration, the soil cross sections of the northwest to southeast direction survey lines orthogonal to the old lake whose displacement distribution were examined in (1) were estimated, and seismic response analysis and residual

deformation were conducted using the soil test results. As a result of the analyses, it was possible to reproduce the deformation that matches the tendency of the horizontal displacement and vertical displacement distribution obtained by SAR.

(4) From these, it is concluded that a caldera lake with a bowl-shaped bottom was once formed in this area, and a special lake deposit containing diatoms and pumice was deposited with a large void ratio, and, due to the earthquake, its shear stiffness decreased sharply and was deformed so as to wrap around the bottom of the old lake. Then, a horizontal tensile force acted on the surface layer near the edge of the old lake, causing grabens.

ACKNOWLEDGMENTS

This research was supported by JSPS KAKENHI Grant Number JP 17H03306 and was carried out with the cooperation of Aso City and residents of the districts where grabens occurred. Dr. Yoshitaka Hase, a former professor at the Graduate School of Kumamoto University, taught us about the characteristics of the Aso Caldera. Dr. Shusaku Ito (Kiso-jiban Consultants Co., Ltd.) provided the geotechnical information based on the soil investigation. The surface wave exploration and reflection survey were conducted by DAIWA Exploration & Consulting Co., Ltd. In addition, the past boring data was provided by the Kyushu Regional Development Bureau of the MLIT, Kumamoto Prefecture, Aso City, and Kyushu Electric Power Co., Inc. The authors are very grateful to these people and institutions.

APPENDIX 1: RESULT OF A STUDY ON THE MECHANISM OF GRABEN THAT OCCURRED IN THE YAKUIMBARU DISTRICT

In the Yakuimbaru district, unlike the four districts of Ozato, Uchinomaki, Kario, and Matoishi, no local displacement occurred according to SAR, and the graben occurred outside the boundaries of the old lake. However, a small river once flowed northward in old topographic maps. A large-scale agricultural land development has been carried out in this area since 1970. The 1/1000 topographic map surveyed at that time by the Aso Land Improvement Agriculture Cooperative is shown in Fig. A1 with the cracks read by GSI. The location of the cracks seemed to coincide with the edge of the old small river, and the subsidence was thought to be due to the soil that filled the small river. In that case, subsidence due to liquefaction and collapse of the cavity that had been formed before the earthquake are considered. Regarding the former, the maximum depth of a small river is about 4 m, and the amount of compression when liquefied is generally about 5% of the layer thickness, so it is difficult to explain the actual subsidence of about 1 m. Regarding the latter, it is said that when burying the small river, stones were laid on the riverbed and soil was placed on the stones. Therefore, it is presumed that the groundwater flowing between the stones gradually caused the soil in the lower part of the buried soil to flow out and form a cavity, and it was thought that a depression occurred due to the earthquake motion there.

APPENDIX 2: DEFORMATION THAT SEEMS TO BE A GRABEN SEEN AT THE KONOBARU ARCHAEOLOGICAL SITE

There have been archaeological sites in the Aso Caldera since the Paleolithic era, but according to Aso City officials, there is no record of ground deformation by past earthquakes. According to the records of past earthquakes, *M*j 6 class earthquakes occurred in August 1894 and February 1895, and north-south tremors were predominant (Kubodera[25]). However, the details are unknown. The *M*j 4.1 and *M*j 4.5 earthquakes that occurred in 1997 and 1999 caused severe damage outside the caldera, but the deformation of this area is unknown. On the other hand, two faults with a strike of N60°E (about 1 m step) were confirmed during the construction of the Kono flood control basin on the east side of Ogaishi Eastern Elementary School in the Kario district[26]. Since the Kumamoto Earthquake caused grabens where these fault lines extended to the west, it is highly possible that these two faults have the same characteristics as graben. Since the investigation revealed that the N2 ash layer that erupted from

Nakadake about 1000 years ago was displaced, it is considered that these faults occurred relatively recently. A fault was also observed in the excavation survey of the Konobaru A site near this construction site[15]. Here, the fault is covered by a soil layer deposited about 1600 years ago.

APPENDIX 3: METHODS FOR SURFACE WAVE EXPLORATION, REFLECTION SURVEY, MICROTREMOR ARRAY OBSERVATION

(1) Surface wave exploration

The equipment used for surface wave exploration was 24 receivers "GS11D" (manufactured by OYO, natural frequency 4.5Hz), one measuring instrument "McSEIS-SW" (manufactured by OYO), one large hammer, and two take-out cables. The measurement was carried out by hitting the ground surface with a large hammer to generate wave oscillations and recording the vibrations with many receivers installed on the survey line. One receiver unit consisted of 24 receivers arranged in a straight line every 2 m. The oscillation was performed on a line (offset) 5 m from the last receiver. The received vibrations were converted into electric signals and recorded by the measuring instrument through the take-out cables. Then, the receiver unit was moved 2 m each time it was oscillated (measured), and the measurement was repeated until the end of the survey line. Data processing and analysis of the measurement results were performed using "SeisImager/SW" (manufactured by OYO) according to the following procedure: i) arrangement of geometry, ii) analysis of cross-correlation, iii) analysis of dispersion curve, and iv) estimation of the initial model and determination of the final model.

(2) Reflection survey

The equipment used for the reflection survey was one hydraulic impactor "JMS-Mini65" (manufactured by JGI), two measuring instruments "Seismic Source DAQ Link III 24ch" (manufactured by Seismic Source), and one PS "Panasonic Toughbook" for control, 48 geophones (28 Hz, manufactured by OYO Geospace), 4 analog signal cables, and one trigger cable. In the exploration, marking was first performed along the survey line at intervals of 5 m from the starting point. Geophones were placed there at intervals of 5 m, then the measuring instruments, analog cables, and trigger cables were put in place. Oscillation was performed at 2.5 m intervals. Data processing and analysis of the measurement results were performed using the seismic exploration processing system "SuperX-C" (manufactured by JGI) according to the following procedure: i) arrangement of geometry, ii) decision of common polymerization points, iii) correction at surface layer, iv) adjusting the amplitude according to the distance, v) correction of waveform, vi) analysis of velocity, vii) NMO correction, viii) CMP polymerization, ix) migration, and x) conversion to depth.

(3) Microtremor array observation

The equipment used for microtremor array observation was a 3-component accelerometer "JU410" (manufactured by Hakusan Corporation) with a built-in GPS, battery and data logger. For observation, six seismometers were used: one was placed in the center of the site, three were placed on the circumference with a radius of 0.6 m (normal array), and two were placed in a triangular position with a side length of 7 to 13 m from the center (irregular array), as shown in Fig. A2. The array analysis tool BIDO[27] was used to analyze the observed results. With this tool, the analysis of the dispersion curve

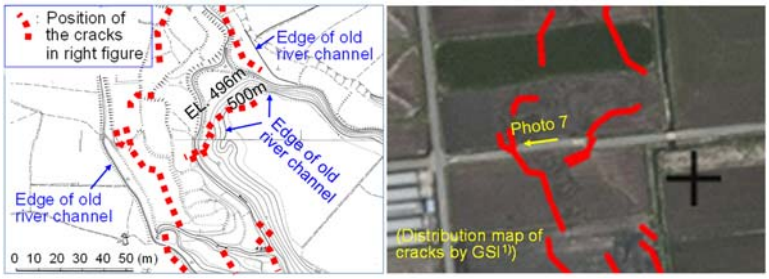

Fig. A1 Position of cracks on old topographic map of the Yakuimbaru district

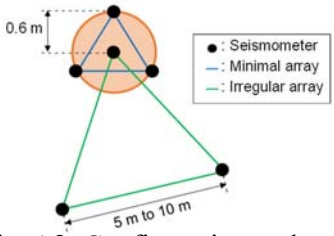

Fig. A2 Configuration and placement of microtremor array observation

can identify the phase velocity in a wider band than the SPAC method by Aki[28] or Okada[29]. Therefore, it was calculated by both this tool and the CCA method[30] and after examining the accuracy of both methods, the final phase velocity result was obtained. In the analysis of the S-wave velocity depth distribution, the Simple Profiling Method (SPM, ex. Ballard[31]) was used to convert the dispersion curve into an S-wave velocity depth distribution by applying a simple conversion formula. The Simplified Inversion Method (SIM) proposed by Pelekis and Athanasopoulos[32] was used for modeling the smooth S-wave velocity distribution in layers. In addition, since three-component microtremors were observed, velocity structure analysis by joint inversion of H/V spectral ratio and phase velocity (Arai and Tokimatsu[33]) was conducted, and the S-wave velocity distribution was calculated so that the results were in harmony with both the periodic characteristics of the ground and the phase velocity.

REFERENCES

1) Geospatial Information Authority of Japan: The 2016 Kumamoto Earthquake, Crack Distribution Map around the Futagawa Fault Zone by Aerial Photo Interpretation (in Japanese, title translated by the authors). http://www.gsi.go.jp/BOUSAI/H27-kumamoto-earthquake-index.html (last accessed on June 30, 2017)
2) Hase, Y., Miyabuchi, Y., Haruta, N., Sasaki, N. and Yumoto, T.: Change of Sedimentary Facies and Topographic Process after the Late Period of the Last Glacial Age of Asodani in the Northern Area of Aso Caldera in Central Kyushu, Japan, *Bulletin of Goshoura Cretaceous Museum*, No. 11, pp. 1–10, 2010 (in Japanese).
3) Kumamoto Geotechnical Consultants Association: Geological Map of Kumamoto Prefecture, 2008 (in Japanese, title translated by the authors).
4) Fujiwara, S., Morishita, Y., Nakano, T., Kobayashi, T. and Yarai, H.: Non-Tectonic Liquefaction-Induced Large Surface Displacements in the Aso Valley, Japan, Caused by the 2016 Kumamoto Earthquake, Revealed by ALOS-2 SAR, *Earth and Planetary Science Letters*, Vol. 474, pp. 457–465, 2017.
5) Tsuji, T., Ishibashi, J., Ishitsuka, K. and Kamata, R.: Horizontal Sliding of Kilometre-Scale Hot Spring Area during the 2016 Kumamoto Earthquake, *Scientific Reports*, Vol. 7, 42947, 2017.
6) Hamada, M., Yasuda, S., Ishoyama, R. and Emoto, K.: Observation of Permanent Ground Displacements Induced by Soil Liquefaction, *Journal of Japan Society of Civil Engineers*, Vol. 376, 3–6, pp. 221–229, 1986 (in Japanese).
7) Yasuda, S., Nagase, H., Kiku, H. and Uchida, Y.: The Mechanism and Simplified Procedure for the Analysis of Permanent Ground Displacement Due to Liquefaction, *Soils and Foundations*, Vol. 32, No. 1, pp. 149–160, 1992.
8) Mimura, C., Yasuda, S., Ohmachi, T., Kawamura, M. and Nakamura, Y.: Geotechnical Damage by the 1985 Mexico Earthquake (Part 2), *Japan Society of Civil Engineers 1986 Annual Meeting*, 3, pp. 35–36, 1986 (in Japanese).
9) Geospatial Information Authority of Japan: The Crustal Movement Caused by the 2016 Kumamoto Earthquake Captured by the Electronic Reference Point (in Japanese, title translated by the authors). https://www.gsi.go.jp/chibankansi/chikakukansi_kumamoto20160414.html (last accessed on April 16, 2016)
10) Shimada, M., Yasuda, S. and Ishikawa, K.: Surface Deformation Measurement for the Kumamoto Earthquake 2016 Using the 3 DinSAR Images Observed by the ALOS-2/PALSAR-2, *The 63rd Autumn Conference of the Remote Sensing Society of Japan*, pp. 145–148, 2017 (in Japanese).
11) Shimada, M.: Imaging from Spaceborne and Airborne SARs, Calibration, and Applications, Chapter 12 SAR Interferometry, CRC-Press, pp. 251–301, 2018.
12) Shimada, M.: Verification Processor for SAR Calibration and Interferometry, *Advances in Space Research*, Vol. 23, No. 8, pp. 1477–1486, 1999.
13) Japan Meteorological Agency: Earthquake Information, 2016. http://www.data.jma.go.jp/svd/eqev/data/kyoshin (last accessed on August 24, 2017)
14) Ishikawa, K. and Yasuda, S.: Ground Displacement Estimated from the Seismic Waveform Observed in Aso Valley During the 2016 Kumamoto Earthquake, *Japan Society of Civil Engineers*

2018 Annual Meeting, 3, pp. 335–336, 2018 (in Japanese).
15) Kumamoto Prefectural Board of Education: Konobaru Archaeological Site, *Kumamoto Prefectural Cultural Property Survey Report*, No. 257, 358 pp. (Vol. 1), 411 p. (Vol. 2), 2010 (in Japanese, title translated by the authors).
16) Yasuda, S., Yoshida, N., Adachi, K., Kiku, H. and Ishikawa, K.: Simplified Evaluation Method of Liquefaction-Induced Residual Displacement, *Journal of Japan Association for Earthquake Engineering*, Vol. 17, No. 6, pp. 1–20, 2017.
17) Ishihara, K.: Soil Behaviour in Earthquake Geotechnics, *Oxford Engineering Science Series*, Oxford University Press, 360 pp., 1996.
18) Taniguchi, E., Kubota, T. and Kuwabara, T.: Slope Failure at Matsukoshi by the Naganoken-Seibu Earthquake, *Tsuchi-To-Kiso*, Vol. 33, No. 11, pp. 59–65, 1985 (in Japanese).
19) Gregersen, O.: The Quick Clay Landslide in Rissa, Norway, *Norwegian Geotechnical Institute Publication*, No. 135, pp. 1–6, 1981.
20) National Research Institute for Earth Science and Disaster Resilience: Strong-Motion Seismograph Networks, 2016. http://www.kyoshin.bosai.go.jp/kyoshin/ (last accessed on August 24, 2017)
21) Yasuda, S. and Yamaguchi, I.: Dynamic Soil Properties for Various Undisturbed Soil Samples, *20th Japan National Conference on Geotechnical Engineering*, pp. 539–542, 1985 (in Japanese).
22) Senna, S., Wakai, A., Yatagai, A, Inagaki, Y., Matsuyama, H. and Fujiwara, H.: Microtremor Array Measurement Results across the Aso Area, *54th Japan National Conference on Geotechnical Engineering*, pp. 1869–1870, 2019 (in Japanese).
23) Smith, W. H. F. and Wessel, P.: Gridding with Continuous Curvature Splines in Tension, *Geophysics*, Vol. 55, No. 3, pp. 293–305, 1990.
24) National Research Institute for Earth Science and Disaster Resilience: Strong Tremors by the April 16, 2016 Earthquake in the Kumamoto Region of Kumamoto Prefecture (in Japanese, title translated by the authors). https://www.kyoshin.bosai.go.jp/kyoshin/topics/Kumamoto_20160416/kumamoto201604160125.pdf (last accessed on August 24, 2017)
25) Kubodera, A. and Miyazaki, M.: Seismic Activity in Kumamoto Prefecture, *Kumamoto Prefecture Earthquake Countermeasures Basic Survey Report*, pp. 31–140, 1981 (in Japanese, title translated by the authors).
26) Sudo, Y. and Ikebe, S.: New Active Fault Descried in Aso Caldera and Seismic Activity, *Disaster Prevention Research Institute Annuals, Kyoto University*, No. 44, B-1, pp. 345–352, 2001 (in Japanese).
27) Cho, I.: Microtremor Analysis Codes BIDO. https://staff.aist.go.jp/ikuo-chou/bidodl.html (last accessed on May 22, 2016)
28) Aki, K.: Space and Time Spectra of Stationary Stochastic Waves, with Special Reference to Microtremors, *Bulletin of the Earthquake Research Institute, University of Tokyo*, Vol. 35, No. 3, pp. 415–456, 1957.
29) Okada, H.: Theory of Efficient Array Observations of Microtremors with Special Reference to the SPAC Method, *Exploration Geophysics*, Vol. 37, No. 1, pp. 73–85, 2006.
30) Cho, I., Senna, S. and Fujiwara, H.: Miniature Array Analysis of Microtremors, *Geophysics*, Vol. 78, No. 1, KS13–KS23, 2013. https://doi.org/10.1190/GEO2012-0248.1
31) Ballard, R. F., Jr.: Determination of Soil Shear Moduli at Depths by In-Situ Vibratory Techniques, *Miscellaneous Paper*, No. 4-691, U.S. Army Engineer Waterways Experiment Station, 1964.
32) Pelekis, P. C. and Athanasopoulos, G. A.: An Overview of Surface Wave Methods and a Reliability Study of a Simplified Inversion Technique, *Soil Dynamics and Earthquake Engineering*, Vol. 31, No. 12, pp. 1654–1668, 2011.
33) Arai, H. and Tokimatsu, K.: S-Wave Velocity Profiling by Joint Inversion of Microtremor Dispersion Curve and Horizontal-to-Vertical (H/V) Spectrum, *Bulletin of the Seismological Society of America*, Vol. 95, No. 5, pp. 1766–1778, 2005. https://doi.org/10.1785/0120040243

(Original Japanese Paper Published: February, 2021)
(English Version Submitted: July 12, 2021)
(English Version Accepted: September 2, 2021)